BIHARBRAINS

Manthan

International Journal of Scientific Research and Innovation
Published Quarterly by B.Brains Scholastic Center
(Under BBrains Development Society)

JUNE 2011 www.bbmanthan.info

Special Issue
4th Bihar Science Conference 2011

Manthan

June, 2011

Contents

ISSN No. 0974-6331, Volume 12

Manthan is an International Journal of Scientific Research and Innovation Published quarterly by B.Brains Scholastic Center (under BBrains Development Society),'*A gyan Kendra'* under the guidance of Global Scientific Council of the society with the objectives of sharing ideas, innovation, knowledge and achievements which can be benefited to the scientific and non-scientific community.

Publishing Office

BBrains Scholastic Center
Malti Niwas, Road No-1, Dhelwa
Near Bus Stand Byepass Road
Kankarbagh, Patna, India
Tel: +91-8002359537

Email : bbmanthan@gmail.com
Web : www.bbmanthan.info

From Editors desk

BBrains Scholastic Center (under BBrains Development Society) organized Fourth International Conference on Science & Technology "Fourth Bihar Science Conference 2011 (BSC 2011)" in association with BRA Bihar University at its LS College, Muzaffarpur (India) from Feb 11 to 13, 2011. The theme of the conference was "Developing attitude of product development and transforming ideas into implementation". On this occasion, around 600 delegates and eminent scientists of from various universities were participated. The highlight of this conference was the inauguration and keynote lecture by Dr. R. K. Pachauri, Director General of TERI and Chairman of IPCC who got Nobel Peace Prize in 2007.

The universities who participated this year are Thammasat University (Thailand), Isik University (Turkey), university of Puebla (Mexico), King Saud University (Riyadh), Massetues Institute of Technology (USA), Chevron (USA), National Polytechnic Institute, (Mexico), CINVESTAV (Mexico), DRDO (Delhi), IIT (Patna), IIT (Delhi), IIT (Kanpur), University of Hyderabad (Hyderabad), Aligarh Muslim University (Aligarh), Gautam Budha university (NOIDA), CFRI (Mumbai), Indian Institute of Packaging (Hyderabad), NIT (Patna), Tata Institute of Fundamental Research (Mumbai), West Bengal University of Science & Technology and all Bihar and Jharkhand based universities etc.

This conference has become forum to help and support research activities of the colleges and universities of Bihar. Since the start of the conference, the research quality and working style of the local scientists has visibly improved.

This SPECIAL 12th Issue of **Manthan** is the supplement of BSC 2011 which covers selected full length papers/ articles of delegates, keynote speakers and young scientist awardees of the said conference.

We solicit your reactions, comments and suggestions in the mailbox and expect that with your help and support in future this magazine will grow into a versatile platform.

For details you are free to visit our website www.bbmanthan.info

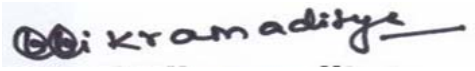

Bibhuti Bikramaditya
Chief Editor

Manthan, International Journal, Vol. 12, June, 2011, Pages 2-8
ISSN No. 0974-6331 www.bbmanthan.info

Finding all Justifications in the SNOMED CT

Boontawee Suntisrivaraporn

School of Information, Computer and Communication Technology
Sirindhorn International Institute of Technology, Thammasat University, Thailand

***Abstract*— SNOMED CT is a large-scale medical ontology, which is developed using a variant of the inexpressive Description Logic $\mathcal{EL}$. Description Logic reasoning can not only be used to compute subsumption relationships between SNOMED concepts, but also to pinpoint the reason why a certain subsumption holds by finding justifications—sets of axioms responsible for this relationship. This helps the ontology developers to understand such a relationship and to debug it if needed. This paper describes an extension to our method of finding "one" justification to a new method that finds "all" justifications for a given subsumption. Our experiments on SNOMED CT show that (i) finding all justifications in this large ontology is practicable and can be done incrementally; and (ii) the number of justifications and their size are manageably small.**

I. INTRODUCTION

Description Logics (DLs) [1] are a familiy of logic-based knowledge representation formalisms, which can be used to develop ontologies (i.e. knowledge bases) in a formally well-founded way. This is true both for expressive DLs, which are the logical basis of the Web Ontology Language OWL 2[1], and for lightweight DLs of the $\mathcal{EL}$ family [2], which are used in the design of large-scale medical ontologies such as SNOMED CT[2] [3] and form one of the W3C-recommended tractable OWL profiles, OWL 2 EL[3]. One of the main advantages of employing a logic-based ontology language is that reasoning services can be used to derive implicit knowledge from the one explicitly represented. DL systems can, for example, classify a given ontology, i.e., compute all the subclass/superclass relationships between the concepts defined in the ontology and arrange these relationships as a hierarchical graph. The advantage of using a lightweight DL of the $\mathcal{EL}$ family is that classification is tractable, i.e., $\mathcal{EL}$ reasoners such as CEL [4] can compute the subclass hierarchy of a given ontology in polynomial time.

Similar to writing large programs, building large-scale ontologies is an error-prone endeavour. Classification can help to alert the developer or user of an ontology to the existence of errors. For example, the subclass relationship between AmputationOfFinger and AmputationOfArm in SNOMED CT is clearly unintended [5], [6], and thus reveals a modelling error. (It means that "any case of amputation of finger is considered as amputation of hand as well.") However, given an unintended subsumption relationship in a large ontology like SNOMED CT with almost 400 000 axioms, it is not always easy to find the erroneous axioms responsible for it by hand. To overcome this problem, the DL community has recently invested quite some work on automating this process. Given a subclass relationship or another questionable consequence, the aim is to find "a justification" or "all justifications" for that consequence, where a justification is a minimal subset of the ontology that has this consequence. Most of the work on axiom pinpointing in DLs was concerned with rather expressive DLs (see, e.g., [7], [8], [16]). The first paper that concentrated on finding justifications in the $\mathcal{EL}$ family of DLs was [9]. In addition to providing complexity results for finding justifications, [9] introduces a "pragmatic" algorithm for computing one justification, which is based on a modified version of the classification algorithm used by the CEL reasoner[4]. Though that approach worked quite well for mid-size ontologies (see the experiments on a variant of the GALEN medical ontology described in [9]), it was not efficient enough to deal with large-scale ontologies like SNOMED CT. The first positive result on finding justifications in SNOMED CT was reported in [10], in which the authors proposed a highly efficient optimization technique based on the computation of a module of the ontology. However, the implemented algorithm in [10] could compute only "one" justification for each subclass relationship.

In this paper, we proposed an extension of that idea and design an algorithm that can effectively and efficiently compute "all" justifications for a given subclass relationship. Empirical results on a large number of random subclass relationships in SNOMED CT are reported which conclusively demonstrate that (i) finding all justifications in the ontology is practicable; and (ii) the number of justifications and their size are manageably small when compared against the size of the ontology.

II. PRELIMINARIES

In this section, we first introduce the description logic (DL) $\mathcal{EL}^+$, which is an extension of the underlying logical formalism of SNOMED CT and which is a logical core of OWL 2 EL Profile.[5] Then, we give the notions of justifications or minimal axiom sets, which lie at the heart of logical explanation support in DL systems.

Like other DLs, an $\mathcal{EL}^+$ signature is the disjoint union $\mathsf{S} = \mathsf{CN} \cup \mathsf{RN}$ of the sets of concept names and role names.

[1] http://www.w3.org/TR/owl2-overview/
[2] Systematized NOmenclature of MEDicine, Clinical Terms.
[3] http://www.w3.org/TR/owl2-profiles/#OWL_2_EL_2
[4] Available at http://cel.googlecode.com
[5] Here, the DL lingo is adopted; it is worthwhile noting that the terms 'concept' and 'role' are known in OWL as 'class' and 'property,' respectively.

Syntax	Semantics
$\top$	$\Delta^{\mathcal{I}}$
$C \sqcap D$	$C^{\mathcal{I}} \cap D^{\mathcal{I}}$
$\exists r.C$	$\{x \in \Delta^{\mathcal{I}} \mid \exists y \in \Delta^{\mathcal{I}} : (x,y) \in r^{\mathcal{I}} \wedge y \in C^{\mathcal{I}}\}$
$C \sqsubseteq D$	$C^{\mathcal{I}} \subseteq D^{\mathcal{I}}$
$r_1 \circ \cdots \circ r_n \sqsubseteq s$	$r_1^{\mathcal{I}} \circ \cdots \circ r_n^{\mathcal{I}} \subseteq s^{\mathcal{I}}$

TABLE I
SYNTAX AND SEMANTICS OF $\mathcal{EL}^+$.

Algorithm 1 Naive computation of "one" justification $\mathcal{S}$ for $A \sqsubseteq_{\mathcal{O}} B$.

function naive-one-just$(A, B, \mathcal{O})$

1: $\mathcal{S} := \mathcal{O}$
2: **for** each axiom $\alpha \in \mathcal{O}$ **do**
3: **if** $A \sqsubseteq_{\mathcal{S}\setminus\{\alpha\}} B$ **then**
4: $\mathcal{S} := \mathcal{S} \setminus \{\alpha\}$
5: **return** $\mathcal{S}$

$\mathcal{EL}^+$ *concept descriptions (or complex concept)* are defined inductively as follows: Concept names $A \in \mathsf{CN}$, the bottom concept $\bot$, and the top concept $\top$ are $\mathcal{EL}^+$ concept descriptions. If C, D are $\mathcal{EL}^+$ concept descriptions and $r \in \mathsf{RN}$ a role name, then conjunction $C \sqcap D$ and existential restriction $\exists r.C$ are also $\mathcal{EL}^+$ concept descriptions. An $\mathcal{EL}^+$ ontology $\mathcal{O}$ is a finite set of axioms of the following forms: general concept inclusion (GCI) $C \sqsubseteq D$, role inclusion $r_1 \circ \cdots r_n \sqsubseteq s$, $\text{DOMAIN}(r) \sqsubseteq C$, and $\text{RANGE}(r) \sqsubseteq C$.For convenience, we write $\mathsf{Sig}(\mathcal{O})$ (resp., $\mathsf{Sig}(\alpha)$, $\mathsf{Sig}(C)$) to denote the signature of the ontology $\mathcal{O}$ (resp., the axiom α, the concept C), i.e., concept and role names occurring in it.

For readability and briefness, the standard set-theoretic semantics is merely summarized in Table I above, and the interested reader is referred to [11], [12] for details. Rather, some intuition is portrayed by means of an example. Fig. 1 depicts a small example of $\mathcal{EL}^+$ ontology $\mathcal{O}_{\mathsf{med}}$ motivated by the medical ontology SNOMED CT. Axioms α_1–α_4 are examples of *primitive concept definitions* which provide only necessary conditions, whereas axioms α_5–α_7 are examples of *(fully defined) concept definitions* which provide both necessary and sufficient conditions. GCIs are typically used to add constraints as in α_{11}, but they also generalize the two types of concept definitions. Role inclusions generalize at least *reflexivity* (α_{12}), *transitivity* (α_{13}), *right-identity* (α_{14}) and *role hierarchy* (α_{15}).

The main inference problem for concepts is *subsumption query*: given an ontology $\mathcal{O}$ and two concept descriptions C, D, check if C is subsumed by (i.e., more specific than; or subclass of) D w.r.t. $\mathcal{O}$, written $C \sqsubseteq_{\mathcal{O}} D$ or $\mathcal{O} \models C \sqsubseteq D$. The identification of subsumption relationships between *all* pairs of concept names occurring in $\mathcal{O}$ is known as *ontology classification*. From $\mathcal{O}_{\mathsf{med}}$, the following subsumptions can be inferred:

$$\mathsf{Appendicitis} \sqsubseteq_{\mathcal{O}_{\mathsf{med}}} \mathsf{HeartDisease} \quad (1)$$

and that:

$$\mathsf{Endocarditis} \sqsubseteq_{\mathcal{O}_{\mathsf{med}}} \mathsf{HartDisease}. \quad (2)$$

The first subclass relation says that "every case of appendicitis has to be considered a heart disease," which is obviously incorrect. This is an example of a false positive inference result. The second subclass relation however is intuitive and intended to be had.

In this paper, we focus on the problem of finding (all) *justifications* as for why a particular subsumption follows from the ontology. Not only are justifications useful in helping to see what goes wrong in the unintended subsumption 1, it also helps to gain insight into the readily correct subsumption 2. To justify a particular subconcept/superconcept relationship, we need to extract core axioms from the ontology, namely those that are necessarily responsible for the relationship in question. To this end, we define the notion of a *justification* or *MinA* as follows:

Definition 1 (Justification). Let $\mathcal{O}$ be an $\mathcal{EL}^+$ ontology, A, B concept names such that $A \sqsubseteq_{\mathcal{O}} B$. Then, a subset $\mathcal{S} \subseteq \mathcal{O}$ is a *minimal axiom set (MinA)* or *justification* for $A \sqsubseteq_{\mathcal{O}} B$ if and only if $A \sqsubseteq_{\mathcal{S}} B$ and, for every $\mathcal{S}' \subset \mathcal{S}$, $A \not\sqsubseteq_{\mathcal{S}'} B$. ◇

With respect to the small ontology $\mathcal{O}_{\mathsf{med}}$, it is not difficult to verify that the only justification for subsumption 1 is $\{\alpha_1, \alpha_5, \alpha_8, \alpha_9, \alpha_{14}\}$. In general, however, justifications may not be unique, and the number of justifications for a particular subsumption may be exponential in the worst case [9]. Subsumption 2, for instance, has two justifications: $\{\alpha_2, \alpha_3, \alpha_6, \alpha_8, \alpha_9, \alpha_{14}\}$ and $\{\alpha_2, \alpha_4, \alpha_6, \alpha_8, \alpha_9, \alpha_{14}\}$. In other words, endocarditis is an inflammation that occurs on endocardium which could be the heart wall *or* the heart valve.

III. MODULARIZATION-BASED APPROACH TO FINDING "ONE" JUSTIFICATION

In $\mathcal{EL}^+$, the problem of finding one justification is tractable [9]. In fact, there is a straightforward algorithm to extract a MinA by going through all the axioms one by one and checking if the subsumption still holds in absence of each of them (see Algorithm 1). Since subsumption checking is polynomial and there are linearly many axioms, this algorithm runs in polynomial time.

With SNOMED, however, this naive approach does not work due to an obvious reason: it requires almost half a million subsumption tests to find a single justification.

To overcome this obstacle, we have proposed a justification finding paradigm based on so-called modularization in [10]. Since this is the basis of the extended paradigm that finds "all" justifications, we summarize it here for completeness. The paradigm essentially comprises two stages as shown in Fig. 2 (*left*): *(i)* extract a module $\mathcal{O}'$ from the ontology $\mathcal{O}$, and then *(ii)* find one justification from the module $\mathcal{O}'$.

Let $\mathcal{O}$ be an $\mathcal{EL}^+$ ontology. Then, a *module* $\mathcal{O}'$ *for a subsumption* σ *in* $\mathcal{O}$ is a subset $\mathcal{O}' \subseteq \mathcal{O}$ such that $\mathcal{O} \models \sigma$ iff $\mathcal{O}' \models \sigma$. A *module* $\mathcal{O}'$ *for a signature* $\mathbf{S} \subseteq \mathsf{Sig}(\mathcal{O})$ *in* $\mathcal{O}$ is a subset $\mathcal{O}' \subseteq \mathcal{O}$ such that, for each subsumption σ with $\mathsf{Sig}(\sigma) \subseteq \mathbf{S}$, $\mathcal{O} \models \sigma$ iff $\mathcal{O}' \models \sigma$. Observe that

α_1				Appendix	$\sqsubseteq$	BodyPart $\sqcap$ $\exists$part-of.Heart
α_2	$\star$	†	‡	Endocardium	$\sqsubseteq$	Tissue $\sqcap$ $\exists$part-of.HeartValve $\sqcap$ $\exists$part-of.HeartWall
α_3	$\star$	†		HeartValve	$\sqsubseteq$	BodyValve $\sqcap$ $\exists$part-of.Heart
α_4	$\star$		‡	HeartWall	$\sqsubseteq$	BodyWall $\sqcap$ $\exists$part-of.Heart
α_5				Appendicitis	$\equiv$	Inflammation $\sqcap$ $\exists$has-location.Appendix
α_6	$\star$	†	‡	Endocarditis	$\equiv$	Inflammation $\sqcap$ $\exists$has-location.Endocardium
α_7				Pancarditis	$\equiv$	Inflammation $\sqcap$ $\exists$has-exact-location.Heart
α_8	$\star$	†	‡	Inflammation	$\sqsubseteq$	Disease $\sqcap$ $\exists$acts-on.Tissue
α_9	$\star$	†	‡	HeartDisease	$\equiv$	Disease $\sqcap$ $\exists$has-location.Heart
α_{10}	$\star$			Tissue $\sqcap$ Disease	$\sqsubseteq$	$\bot$
α_{11}				HeartDisease $\sqcap$ $\exists$causative-agent.Virus	$\sqsubseteq$	ViralDisease $\sqcap$ $\exists$has-state.NeedsTreatment
α_{12}	$\star$			ϵ	$\sqsubseteq$	part-of
α_{13}	$\star$			part-of $\circ$ part-of	$\sqsubseteq$	part-of
α_{14}	$\star$	†	‡	has-location $\circ$ part-of	$\sqsubseteq$	has-location
α_{15}				has-exact-location	$\sqsubseteq$	has-location

Fig. 1. An example $\mathcal{EL}^+$ ontology $\mathcal{O}_{\text{med}}$. $\star$ denote the axioms in the module with signature {Endocarditis}, whereas † and ‡ denote the axioms in the two justifications for Endocarditis $\sqsubseteq_{\mathcal{O}_{\text{med}}}$ HartDisease.

this is a very generic definition, in the sense that the whole ontology is itself a module. We are however interested in certain sufficient conditions that not only give us a module, but also guarantee relevancy of extracted axioms. Here, we consider the *reachability-based module* which has been first introduced in [13]:

Definition 2 (Reachability-based modules). Let $\mathcal{O}$ be an $\mathcal{EL}^+$ ontology, $\mathbf{S} \subseteq \text{Sig}(\mathcal{O})$ a signature, and $x, y \in \text{Sig}(\mathcal{O})$ concept or role names. We say that x is *connectedly reachable* from $\mathbf{S}$ w.r.t. $\mathcal{O}$ (for short, *reachable* from $\mathbf{S}$ or $\mathbf{S}$-*reachable*) iff $x \in \mathbf{S}$ or there is an axiom (either GCI or RI) $\alpha_L \sqsubseteq \alpha_R \in \mathcal{O}$ s.t. $x \in \text{Sig}(\alpha_R)$ and, for all $y \in \text{Sig}(\alpha_L)$, y is reachable from $\mathbf{S}$.

We say that an axiom $\beta_L \sqsubseteq \beta_R$ is *reachable* from $\mathbf{S}$ w.r.t. $\mathcal{O}$ (for short, $\mathbf{S}$-*reachable*) if, for all $x \in \text{Sig}(\beta_L)$, x is $\mathbf{S}$-reachable. *The reachability-based module* for $\mathbf{S}$ in $\mathcal{O}$, denoted by $\mathcal{O}_{\mathbf{S}}^{\text{reach}}$, is the smallest set of all axioms in $\mathcal{O}$ that are $\mathbf{S}$-reachable, i.e. $\mathcal{O}_{\mathbf{S}}^{\text{reach}} = \{\alpha \in \mathcal{O} | \alpha \text{ is } \mathbf{S}\text{-reachable in } \mathcal{O}\}$. ◇

In [13], it has been shown that, in order to query subsumption $A \sqsubseteq B$ against an ontology $\mathcal{O}$, it suffices to consider axioms in the reachability-based module $\mathcal{O}_A^{\text{reach}}$ for $\mathbf{S} = \{A\}$. Moreover, it has been shown empirically that such modules are generally very small compared to the ontology and that it is very cheap to extract them (see [12] for extensive modularization results on SNOMED).

There is a connection between modules and justifications, in the case where the subsumption holds. Given an ontology $\mathcal{O}$ and concept names A, B such that $A \sqsubseteq_{\mathcal{O}} B$; then, $A \sqsubseteq_{\mathcal{O}_A^{\text{reach}}} B$. It immediately implies that there is a minimal subset $\mathcal{S} \subseteq \mathcal{O}_A^{\text{reach}} \subseteq \mathcal{O}$ such that $A \sqsubseteq_{\mathcal{S}} B$ and, for every $\mathcal{S}' \subset \mathcal{S}$, $A \not\sqsubseteq_{\mathcal{S}'} B$. Obviously, such a minimal subset $\mathcal{S}$ of $\mathcal{O}_A^{\text{reach}}$ is a justification for $A \sqsubseteq_{\mathcal{O}} B$. Algorithm 2 summarizes

Algorithm 2 Modularization-based computation of "one" justification $\mathcal{S}$ for $A \sqsubseteq_{\mathcal{O}} B$.

function mod-one-just$(A, B, \mathcal{O})$

1: $\mathcal{O}_A^{\text{reach}} \leftarrow$ extract-module$(\mathcal{O}, \{A\})$
2: **return** naive-one-just$(A, B, \mathcal{O}_A^{\text{reach}})$

function extract-module$(\mathcal{O}, \mathbf{S})$

1: $\mathcal{O}_{\mathbf{S}} \leftarrow \emptyset$
2: queue $\leftarrow$ active-axioms$(\mathbf{S})$
3: **while not** empty(queue) **do**
4: $(\alpha_L \sqsubseteq \alpha_R) \leftarrow$ fetch(queue)
5: **if** Sig$(\alpha_L) \subseteq \mathbf{S} \cup$ Sig$(\mathcal{O}_{\mathbf{S}})$ **then**
6: $\mathcal{O}_{\mathbf{S}} \leftarrow \mathcal{O}_{\mathbf{S}} \cup \{\alpha_L \sqsubseteq \alpha_R\}$
7: queue $\leftarrow$ queue $\cup$ (active-axioms(Sig$(\alpha_R)) \setminus \mathcal{O}_{\mathbf{S}}$)
8: **return** $\mathcal{O}_{\mathbf{S}}$

the proposed justification finding paradigm that allows CEL to be able to find a justification.

From the example in Fig. 1, the reachability-based module for $\mathbf{S} = \{\text{Endocarditis}\}$ contains α_2, α_3, α_4, α_6, α_8, α_9, α_{10}, α_{12}, α_{13}, α_{14}, and it can be verified that the two justifications for subsumption (2) are indeed covered by this module.

IV. Modularization-Based Approach to Finding "All" Justifications

The paradigm essentially comprises two stages as shown in Fig.2: *(i)* extract a module $\mathcal{O}'$ from the ontology $\mathcal{O}$, and then *(ii)* find "all" justifications from the module $\mathcal{O}'$. Clearly, in order for this paradigm to be complete, i.e. all existing justifications can be found, the module has to cover all the justifications. To this end, we have shown that the reachability-based module has precisely this coverage property, and thus it suffices to consider only axioms in the module and ignore

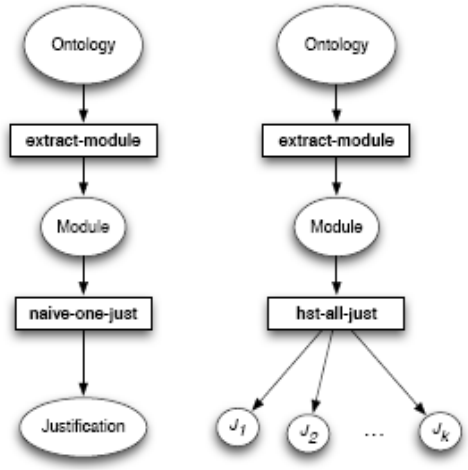

Fig. 2. The modularization-based paradigm for finding one justification (*left*) and all justifications (*right*).

those other axioms when "all" justifications have to be computed.

Lemma 3 ($\mathcal{O}_A^{\text{reach}}$ contains all MinAs for $A \sqsubseteq_\mathcal{O} B$). *Let $\mathcal{O}$ be an $\mathcal{EL}^+$ ontology, A, B concept names such that $A \sqsubseteq_\mathcal{O} B$, and $\mathcal{O}_A^{\text{reach}} \subseteq \mathcal{O}$ the reachability-based module for $\mathbf{S} = \{A\}$. Then, $\mathcal{S} \subseteq \mathcal{O}_A^{\text{reach}}$, for all MinAs $\mathcal{S}$ for $A \sqsubseteq_\mathcal{O} B$.*

This lemma suggests that the proposed paradigm in Fig. 2 (*right*) is complete in the sense that no justifications, if any, will be missed out. The paradigm then applies a modification of the known *hitting set tree (HST) algorithm* by Reiter [14], as well as some optimization techniques proposed in [15].

The intuition behind this algorithm is to attempt to remove some axioms found in the already known justifications to see if the subsumption still holds. If this is affirmative, it clearly means that another justification not containing those removed axioms must exist. This justification must be different from all the known ones since it does away with some axioms found in them, and thus can be extracted by using, for instance, Algorithm 1.

Algorithm 3 describes in detail the pinpointing algorithm based on HST expansion. In the procedure hst-all-justs, two global variables $\mathbf{C}$ and $\mathbf{H}$ are declared and initialized with $\emptyset$. They are used throughout the HST expansion to store the computed justifications and hitting sets, respectively. In line 2, a first justification $\mathcal{S}$ is computed in the usual way by Algorithm 1. Branches from the root are spawned by calling the recursive procedure expand-hst for every axiom $\alpha \in \mathcal{S}$ (line 4–5). Line 1 to 5 of expand-hst implement two optimizations for the HST algorithms [14], [15], [16] that help reduce the size of the HST and minimize calls to the subprocedure naive-one-just.

a) Early path termination: An HST branch can be pruned if a *similar* one has been considered earlier. Here, similarity is determined by the set of removed axioms or the

Algorithm 3 Hitting set tree (HST) pinpointing algorithm.

Procedure hst-all-justs$(A, B, \mathcal{O})$
Input: A, B: concept names; $\mathcal{O}$: $\mathcal{EL}^+$ ontology
Output: collection $\mathbf{C}$ of all justifications for $A \sqsubseteq_\mathcal{O} B$

1: **Global** : $\mathbf{C}, \mathbf{H} := \emptyset$
2: $\mathcal{S} :=$ naive-one-just$(A, B, \mathcal{O})$
3: $\mathbf{C} := \{\mathcal{S}\}$
4: **for** each axiom $\alpha \in \mathcal{S}$ **do**
5: expand-hst$(A, B, \mathcal{O}\backslash\{\alpha\}, \{\alpha\})$
6: **return** $\mathbf{C}$

Procedure expand-hst$(A, B, \mathcal{O}, H)$
Input: A, B: concept names; $\mathcal{O}$: $\mathcal{EL}^+$ ontology; H: list of edge labels
Side effects: modifications to $\mathbf{S}$ and $\mathbf{H}$

1: **if** there exists some $H' \in \mathbf{H}$ such that $H' \subseteq H$ **or** H' contains a prefix-path P with $P = H$ **then**
2: **return** *(early path termination ⊗)*
3: **if** there exists some $\mathcal{S} \in \mathbf{C}$ such that $H \cap \mathcal{S} = \emptyset$ **then**
4: $\mathcal{S}' := \mathcal{S}$ *(justification reuse)*
5: **else**
6: $\mathcal{S}' :=$ naive-one-just$(A, B, \mathcal{O})$
7: **if** $\mathcal{S}' \neq \emptyset$ **then**
8: $\mathbf{C} := \mathbf{C} \cup \{\mathcal{S}'\}$
9: **for** each axiom $\alpha \in \mathcal{S}'$ **do**
10: expand-hst$(A, B, \mathcal{O}\backslash\{\alpha\}, H \cup \{\alpha\})$
11: **else**
12: $\mathbf{H} := \mathbf{H} \cup \{H\}$ *(normal termination ⊙)*

hitting set H.

b) Justification reuse: A known justification $\mathcal{S}$ can be reused in the current HST brach if it does not use any of the removed axioms, i.e. $\mathcal{S}$ and H are disjoint.

To understand hst-all-justs and expand-hst, consider a small ontology $\mathcal{O}_2$ comprising 5 axioms:

$$\begin{array}{llll} \alpha_1: & A \sqsubseteq P_1 \sqcap Q_1, & & \\ \alpha_2: & P_1 \sqsubseteq P_2 \sqcap Q_2, & \alpha_4: & P_2 \sqsubseteq B, \\ \alpha_3: & Q_1 \sqsubseteq P_2 \sqcap Q_2, & \alpha_5: & Q_2 \sqsubseteq B; \end{array}$$

and entailing the subsumption $\sigma = (A \sqsubseteq B)$. There are 4 justifications for σ in $\mathcal{O}_2$. Figure 3 demonstrates the process of computing all justifications by Algorithm 3. To begin with, $\mathcal{O}_2$ is pruned by naive-one-just to obtain the first justification $\{\alpha_1, \alpha_2, \alpha_4\}$, which is the label of the root node n_0 of the HST. The first branch terminates immediately since $\mathcal{O}_2\backslash\{\alpha_1\}$ does not entail σ (marked by $\odot$ in n_1). On the other hand, $\mathcal{O}_2\backslash\{\alpha_2\} \models \sigma$, and the second justification $\{\alpha_1, \alpha_3, \alpha_4\}$ can be computed by pruning $\mathcal{O}_2\backslash\{\alpha_2\}$ which labels n_2. This process continues to expand HST until it finds all other justifications for σ.

Finally, we apply reachability-based modularization to Algorithm 3 to obtain the optimized method for finding all justifications, see Algorithm 4. The method is highly effective on SNOMED CT since the large search space given by all the

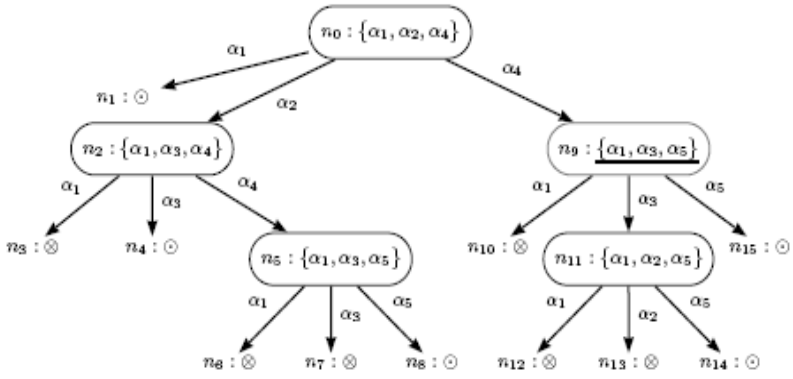

Fig. 3. The hitting set tree produced by Algorithm 3 on the example ontology $\mathcal{O}_2$.

Algorithm 4 Modularization-based computation of "one" justification $\mathcal{S}$ for $A \sqsubseteq_{\mathcal{O}} B$.

function mod-all-justs$(A, B, \mathcal{O})$

1: $\mathcal{O}_A^{\text{reach}} \leftarrow$ extract-module$(\mathcal{O}, \{A\})$
2: **return** hst-all-justs$(A, B, \mathcal{O}_A^{\text{reach}})$

axioms in this medical ontology is drastically reduced to a much smaller module.

V. Experimental Results

We have implemented the proposed modularization-based algorithms by using CEL [4] as the subsumption oracle required in Algorithm 1 which is a sub-procedure for Algorithm 4. The implemented algorithm is tested using a DL version of SNOMED CT, which contains 379,691 concept names and 62 role names. It is an $\mathcal{EL}^+$ ontology with 379,704 axioms, 13 of which are role axioms. Henceforth, we refer to this $\mathcal{EL}^+$ ontology as $\mathcal{O}^{\text{SNOMED}}$. All experimental results presented in the paper have been carried out on and measured by a PC with 2.40 GHz Pentium-4 processor and 1 GB of memory.

To get a grip of what results we may expect to achieve, some previous results [10] w.r.t. finding "one" justifications in $\mathcal{O}^{\text{SNOMED}}$ are summarized here for reference. Based on a false positive subsumption in $\mathcal{O}^{\text{SNOMED}}$, naive-one-just failed to produce an output in 24 hours, whereas mod-one-just took less than a second to find a justification which comprises only 6 axioms. This highly effective optimization technique stems from the fact that the module contains only 57 axioms, as opposed to hundreds of thousands in $\mathcal{O}^{\text{SNOMED}}$. Sizes of modules in $\mathcal{O}^{\text{SNOMED}}$, as well as of justifications (MinAs), are presented in Fig. 4. On average the reachability-based modules are *four orders of magnitude* smaller than the original ontology. For details on modularization experimental results, see [13]. Observe that, though modules in SNOMED are relatively small, the actual sizes of justifications are much smaller. On average, the justification size is 13.36% that of modules. As easily visible from the chart, the majority of

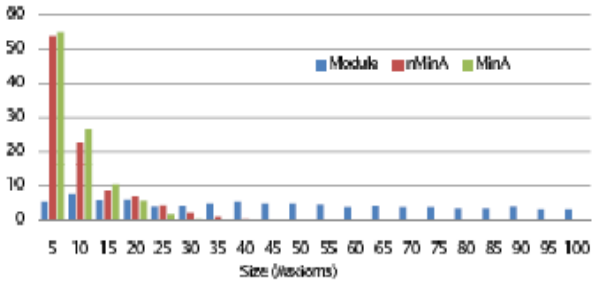

Fig. 4. Relative frequency of the sizes of modules, nMinAs and MinAs for the sampled subsumptions in $\mathcal{O}^{\text{SNOMED}}$.

subsumptions (78%) have a justification of size ten or less axioms.

Here, we focus on the experimental results of finding "all" justifications in $\mathcal{O}^{\text{SNOMED}}$. We sampled 18,673 subsumption relationships that are well-distributed and representative of hard cases. To obtain meaningful testing results, we consider only those subsumption consequences known to have *strictly more than one justification*.[6]

Among the sampled subsumptions are hard cases with more than 100 justifications. Despite the optimizations, the constructed hitting set tree was very large, and it took more than 24 hours and up to 72 hours to compute all justifications. For this reason, the number of computed justifications was limited in our experiment to 10, and the samples would therefore be divided into two groups, namely, easy-samples which comprises subsumptions having between 2 and 9 justifications; and hard-samples which comprises subsumptions having at least 10 justifications.

Based on all the subsumptions considered, 10 492 (56.19%) subsumptions belong to easy-samples, and 8 181 (43.81%) subsumptions to hard-samples. Table II shows the average/maximum numbers of justifications (♯Justs) and their size.

[6]It is worth noting that the majority of subsumptions have only one subsumption, and experiment results on them have been reported in [10].

Samples	♯Justs (avg/max)	Justification size (avg/max)	♯Common ax. (μ)	♯All ax. (ν)	μ/ν
easy-samples (56.19%)	3.74 / 9	8.02 / 26	4.77 / 22	12.30 / 39	0.39
hard-samples (43.81%)	10 / 10	16.39 / 45	7.01 / 30	32.53 / 63	0.22

TABLE II
STATISTICAL RESULTS ON THE COMPUTED JUSTIFICATIONS IN $\mathcal{O}^{\text{SNOMED}}$.

Samples	Time to extract module $\mathcal{O}_A^{\text{SNOMED}}$ (avg/max)	HST search time excl. subs. calls (avg/max)	♯Subs. calls (avg/max)	Total subs. testing time (avg/max)
easy-samples	0.01 / 2.06	0.07 / 44.08	177.60 / 4 732	8.80 / 151.97
hard-samples	0.02 / 3.96	0.09 / 39.90	769.98 / 4 308	37.77 / 375.68

TABLE III
TIME RESULTS (SECOND) OF THE MODULARIZATION-BASED HST PINPOINTING ALGORITHM ON $\mathcal{O}^{\text{SNOMED}}$.

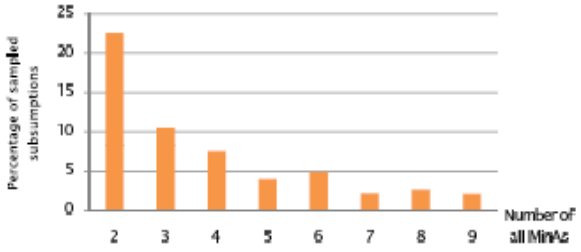

Fig. 5. Relative frequency of the numbers of *all* MinAs for easy-samples in $\mathcal{O}^{\text{SNOMED}}$.

It also presents the average/maximum numbers of common axioms in all justifications, i.e., $\mu = |\bigcap_{\text{justifications } \mathcal{S} \text{ for } \sigma} \mathcal{S}|$, and those of all axioms in all justifications, i.e., $\nu = |\bigcup_{\text{justifications } \mathcal{S} \text{ for } \sigma} \mathcal{S}|$. The average ratio μ/ν, which indicates the degree of commonality of the computed justifications, is shown in the last column of the table. The relative distribution of ♯Justs below ten is shown in Figure 5. More than half of all the considered subsumptions (51.51%) have 7 justifications or less, i.e., the median of ♯Justs for easy-samples and hard-samples collectively is 7. Though nothing can be said about the distribution of ♯Justs larger than 9, it is known from the test results that about 43% have ten or more justifications and that the largest known ♯Justs is 158.

Recall that our proposed algorithm consists of three core computing components: module extraction, hitting set tree construction, and subsumption testing (see Algorithm 3 and 4). A breakdown of runtime for these parts, as well as the number of subsumption calls, is summarized in Table III. The average time to compute all justifications (the first 10 justifications, respectively) using the modularization-based HST pinpointing algorithm was 8.88 seconds (37.88 seconds, respectively). One of the advantages of this algorithm is that it computes the first justification in less than half a second and generates next justifications one after the other. This means that, while the computation is being carried out, partial outputs, i.e., some justifications, are readily available for inspection by the ontology developer. An excessively long computation of all justifications in certain "hard" cases can be interrupted when the developer has enough information for debugging.

REFERENCES

[1] F. Baader, D. Calvanese, D. McGuinness, D. Nardi, and P. Patel-Schneider, editors. *The Description Logic Handbook: Theory, Implementation and Applications*. Cambridge University Press, second edition, 2007.

[2] F. Baader, S. Brandt, and C. Lutz. Pushing the $\mathcal{EL}$ envelope. In *Proceedings of the 19th International Conference on Artificial Intelligence (IJCAI-05)*, Edinburgh, UK, 2005. Morgan-Kaufmann Publishers.

[3] M.Q. Stearns, C. Price, K.A. Spackman, and A.Y. Wang. SNOMED clinical terms: Overview of the development process and project status. In *Proceedings of the 2001 AMIA Annual Symposium*, pages 662–666. Hanley&Belfus, 2001.

[4] F. Baader, C. Lutz, and B. Suntisrivaraporn. CEL—a polynomial-time reasoner for life science ontologies. In U. Furbach and N. Shankar, editors, *Proceedings of the 3rd International Joint Conference on Automated Reasoning (IJCAR'06)*, volume 4130 of *Lecture Notes in Artificial Intelligence*, pages 287–291. Springer-Verlag, 2006.

[5] B. Suntisrivaraporn, F. Baader, S. Schulz, and K. Spackman. Replacing SEP-triplets in SNOMED CT using tractable Description Logic operators. In Jim Hunter Riccardo Bellazzi, Ameen Abu-Hanna, editor, *Proceedings of the 11th Conference on Artificial Intelligence in Medicine (AIME'07)*, volume 4594 of *Lecture Notes in Computer Science*, pages 287–291. Springer-Verlag, 2007.

[6] U. Hahn S. Schulz, K. Mark. Spatial location and its relevance for terminological inferences in bio-ontologies. *BMC Bioinformatics*, 2007.

[7] S. Schlobach and R. Cornet. Non-standard reasoning services for the debugging of Description Logic terminologies. In Georg Gottlob and Toby Walsh, editors, *Proceedings of the 17th International Conference on Artificial Intelligence (IJCAI-03)*, pages 355–362, Acapulco, Mexico, 2003. Morgan-Kaufmann Publishers.

[8] T. Meyer, K. Lee, J. Pan, and R. Booth. Finding maximally satisfiable terminologies for the Description Logic $\mathcal{ALC}$. In *Proceedings of the 21st National Conference on Artificial Intelligence (AAAI'06)*, pages 269–274, 2006.

[9] Franz Baader, Rafael Peñaloza, and Boontawee Suntisrivaraporn. Pinpointing in the description logic $\mathcal{EL}^+$. In *Proceedings of the 30th German Conference on Artificial Intelligence (KI2007)*, LNAI, Osnabrück, Germany, 2007. Springer.

[10] F. Baader and B. Suntisrivaraporn. Debugging SNOMED CT using axiom pinpointing in the Description Logic $\mathcal{EL}^+$. In *Proceedings of the 3rd Knowledge Representation in Medicine Conference (KR-MED'08): Representing and Sharing Knowledge Using* SNOMED, Phoenix AZ, USA, 2008.

[11] F. Baader, C. Lutz, and B. Suntisrivaraporn. Is tractable reasoning in extensions of the Description Logic $\mathcal{EL}$ useful in practice? *Journal of Logic, Language and Information, Special Issue on Method for Modality (M4M)*, 2007.

[12] Boontawee Suntisrivaraporn. *Polynomial-Time Reasoning Support for Design and Maintenance of Large-Scale Biomedical Ontologies*. PhD thesis, TU Dresden, Institute for Theoretical Computer Science, Germany, 2009.

[13] B. Suntisrivaraporn. Module extraction and incremental classification: A pragmatic approach for $\mathcal{EL}^+$ ontologies. In Sean Bechhofer, Manfred Hauswirth, Joerg Hoffmann, and Manolis Koubarakis, editors, *Proceedings of the 5th European Semantic Web Conference (ESWC'08)*, volume 5021 of *Lecture Notes in Computer Science*, pages 230–244. Springer-Verlag, 2008.

[14] R. Reiter. A theory of diagnosis from first principles. *Artificial Intelligence*, 32(1):57–95, 1987.

[15] R. Greiner, B.A. Smith, and R.W. Wilkerson. A correction to the algorithm in reiter's theory of diagnosis. *Readings in model-based diagnosis*, pages 49–53, 1992.

[16] A. Kalyanpur, B. Parsia, M. Horridge, and E. Sirin. Finding all justifications of OWL DL entailments. In *Proceedings of the 6th International Semantic Web Conference (ISWC'07)*, pages 267–280, 2007.

Corresponding Author:
Email: sun@siit.tu.ac.th

Manthan, International Journal, Vol. 12, June, 2011, Pages 9-11
ISSN No. 0974-6331 www.bbmanthan.info

Structural, Magnetic and Mössbauer Studies of Nanocrystalline Ni-Zn Ferrite, Synthesized using Citrate Precursor Method

Rakesh Kumar Singh [a], A. Narayan [b], A. Yadav [c], S.Layek [d]

[a]Department of Physics, Patna Women's College, Patna University, Patna, Bihar, India
[b]Department of Physics, Patna University, Patna, Bihar, India
[c]Vidyavihar Institute of Technology, Purnea, Bihar, India
[d] Department of Physics, IIT Kanpur, Kanpur, India

Abstract

Nanocrystalline Nickel Zinc Ferrite particles ($Ni_xZn_{1-x}Fe_2O_4$) with different composition were prepared by Citrate precursor method. The ferrite powders were characterized using X-ray diffraction (XRD), Vibrating sample magnetometer (VSM) and Mossbauer Spectroscopy tools. The maximum value of saturation magnetization was observed as 52.18 emu/g and Coercivity as 116.10 Oe in sample with x = 0.8. The Mössbauer spectroscopy results show two environments for iron nuclei. In contrast to bulk Ni-Zn ferrites, the lattice parameter in our samples has a tendency to nonlinearly decrease with increase in the proportion of Nickel. The range of average particle size is 7 nm to 18 nm as obtained from XRD line broadening.

Keywords: Ferrite, Nanoparticle, Magnetic Properties, Mossbauer studies

Introduction

Nanocrystalline Spinel Nickel zinc ferrites have been investigated extensively in recent years because of their potential applications in various electronics devices, radio frequency circuits, high quality filters, rod antennas, transformers, read-write heads for high speed digital tape recorders and magnetic storage devices[1,2,3]. Their multifarious use in electronics industry stems from the fact that they have large permeability even at high frequency[4]. Moreover, they have remarkably high electrical resistivity, mechanical hardness, chemical stability and reasonable cost. Several researchers have used citrate precursor method for synthesis of ferrites in bulk as well as nano sizes due to its attractive features like low cost and ease of preparation[5-11]. We have also used the same method for preparing our samples.

Materials and methods

Synthesis of Ni-Zn Ferrite Nanoparticles: Samples of nanometer-sized nickel-zinc ferrite powder, $Ni_xZn_{1-x}Fe_2O_4$(x=0.2, 0.4, 0.5, 0.6, 0.8) were prepared by using the Citrate precursor method. Ferric nitrate, nickel nitrate and Zinc nitrate were taken in stoichiometric proportions as starting materials. Aqueous solutions of these salts were prepared separately by dissolving the salt in minimum amount of deionized water while stirring constantly. The solutions were then mixed together. Aqueous solution of citric acid was prepared in adequate quantity by weight and was added to the prepared salt solutions. The mixture was heated at temperature about 60°C to 80°C for two hours with continuous stirring. This solution was allowed to cool to room temperature and finally it was dried at 90-95°C in an oven until it formed a brown color fluffy mass. This precursor was heated at 450°C for one hour in a muffle furnace. By this process, the precursor decomposed to give nickel-zinc ferrite powder consisting of nanometer size particles.

Results and Discussions

Structural features: The ferrite samples prepared as described above were structurally characterized using large angle X-Ray Diffractometer (XRD). In all our samples of Ni-Zn mixed ferrites, XRD patterns show diffraction peaks that correspond to spinel ferrites mainly, together with small peaks of Hematite (Figure 1) and sodium Zincate tetrahydrate. However, the intensities corresponding to these impurity phases are small. Similar peaks were also observed in Ni-Zn ferrite samples prepared using hydrothermal technique[4]. Albuquerque et al. (2000) have prepared ferrite samples by coprecipitation technique with heat treatment at 300°C as well as higher temperatures[12] and it was shown that samples exhibit good structural ordering only for heat treatment at temperature higher than 400°C. The other phases (in addition to spinel) may be attributed to inaccuracy in stoichiometric proportions, inhomogeneity at microscopic scale and presence of unreacted chemicals in the finished product.

The lattice constant was observed to change with the proportion of nickel. Apart from the anomalous result for x= 0.2, as the proportion of nickel is increased from x= 0 to 0.8, the lattice constant shows a

Manthan, International Journal, Vol. 12, June, 2011, Pages 9-11
ISSN No. 0974-6331 www.bbmanthan.info

decreasing trend. A similar trend has also been reported for bulk nickel-zinc ferrite materials earlier [13].

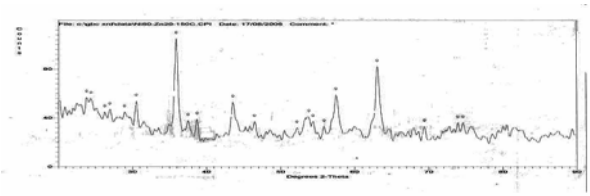

Fig.1: XRD pattern for $Ni_{0.8}Zn_{0.2}Fe_2O_4$ Nanomaterials

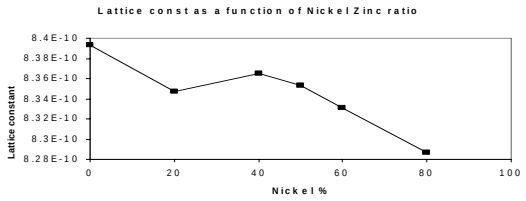

Fig. 2: Variation of Lattice constant with percentage increase of Nickel

Magnetic and Mossbauer studies: The ferrite samples were magnetically characterized using VSM as well as by Mössbauer spectroscopy. The magnetic parameters obtained from VSM measurements of the six samples of Ni-Zn mixed ferrite particles are tabulated in Table 1. The magnetic hysteresis curves for $Ni_{0.8}Zn_{0.2}Fe_2O_4$ nanoparticles are shown in figure 3.

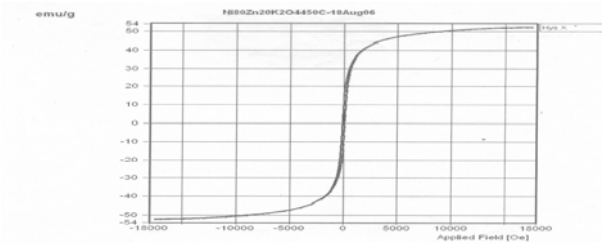

Fig. 3: Hysteresis Loop for $Ni_{0.8}Zn_{0.2}Fe_2O_4$ Nanoparticles

The values of the magnetization parameters do not show a systematic trend with change in composition. Partly the impurity phases and partly the varying particle size might be responsible for this. The annealing temperature of 450^0 C may not be optimum for all the samples. The most interesting case seems to be with $Ni_{0.8}Zn_{0.2}Fe_2O_4$,where both the coercive field (116.10 Oe) and the saturation magnetization (52.18 emu/g) are largest. Values of saturation magnetization higher than 50 emu/g have so far been achieved by using other methods[14,15], only through sintering at temperatures much above 450^oC, the sintering temperature used in the present method. Synthesing ferrite samples at lower temperatures have its own advantages as the grain growth is checked and one is more likely to get strain-free nanoparticles.

Table 1: Magnetic parameters of the Nickel Zinc Ferrite samples

Sample	H_c (Oe)	M_r (emu/g)	M_s (emu/g)	Squareness/ Particle size (nm)
$Ni_{0.2}Zn_{0.8}Fe_2O_4$.	22.42	0.5744	17.50	0.033/ 16
$Ni_{0.4}Zn_{.6}Fe_2O_4$	1.53	0.1049	43.43	0.002/7
$Ni_{0.5}Zn_{0.5}Fe_2O_4$	90.86	5.658	40.54	0.140/16
$Ni_{0.6}Zn_{0.4}Fe_2O_4$	35.77	2.678	43.64	0.059/9
$Ni_{0.75}Zn_{0.25}Fe_2O_4$	93.10	4.610	38.94	0.118/9
$Ni_{0.8}Zn_{0.2}Fe_2O_4$	**116.10**	**11.38**	**52.18**	**0.148/18**

Caizer and Stefaneseu[15] have reported that the magnetic properties are determined by the size of the nanocrystallites. The decrease in saturation magnetisation with decrease in particle size of the nanocrystallites can be attributed to surface effect, spin canting and broken exchange bonds[16]. In our studies, we have also obtained lowering of saturation magnetization as compared to bulk values.

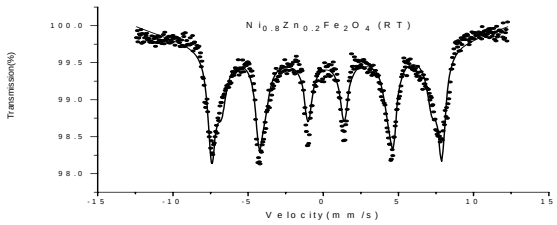

Fig. 4: Mössbauer Spectrum for $Ni_{0.8}Zn_{0.2}Fe_2O_4$ Nanomaterials

The Mössbauer pattern of the $Ni_{0.8}Zn_{0.2}Fe_2O_4$ sample (Fig. 4) shows that two sextets are superposed, one over the other. Ni-ferrite is an inverse ferrite and one expects Fe ions to occupy both A and B sites. Zn has a preference for A-sites and hence the area corresponding to the A-site sextet should be somewhat smaller to that corresponding to B-site. The well resolved six-line pattern shows that there are no significant superparamagnetic fluctuations of the magnetic moment. However, the B_{hf} values of the sextets in the spectrum (47.6 T and 43.5 T) are less than the values expected for bulk samples (50 T to 55 T) indicating the fact that the particles are in nanosize but the blocking temperature is above room temperature. The XRD peak broadening for this particular sample gives the average particle size to be 18 nm consistent with the reduced B_{hf}.

Conclusion

We used a single annealing temperature for all our samples of nanocrystalline Ni-Zn mixed ferrite. We observed that the magnetic properties as well as particle size depended on stoichiometric proportion of

Nickel and Zinc. The maximum saturation magnetization was found to 52.18 emu/g. This might be a feature of the citrate precursor method that was used by us. The lattice parameter has a tendency to decrease with increase in the proportion of Nickel but we did not get a straight line function as has been reported for the case of bulk ferrites. The Mössbauer spectrum shows that Fe occupies both the A and B sites in the sample and superparamegnetic fluctuations are not significant.

Acknowledgement

Authors, Rakesh K. Singh and A. Yadav are thankful to Nalanda Open University, Patna for partial financial support for this work. We are grateful to Prof. H. C. Verma, Dept. of Physics, IIT Kanpur for fruitful discussion and encouragement.

References

[1] Sugimoto, M., J.Am. Ceram. Soc. 82 (1999) 269.
[2] Ishino, K. and Y. Naruniya, Ceram. Bull. 66, (1987) 1469.
[3] Gilot, B., Euro, Phys. J. Appl. Phys. 91 (2002) 10.
[4] Upadhaya, C., D. Mishra, H. C. Verma, S. Anand, R.P. Das, J. Magn. Mag. Mat. 260 (2003) 188.
[5] Guaita, F. J., H. Beltron, E Cordoncillo, J. B.Carda, P.Secribano, J. Euro. Ceram. Soc. 19 (1999) 363.
[6] Vijayalakshmi, A. and N.S. Gajbhiye, J. Appl. Phys. 83 (1998) 400.
[7] Kamble R.C. et al., J. Alloy. Comp., 491 (2010) 372.
[8] Costa, A.C.F.M, Tortella, E, M. R. Morelli, R.H.G.A. Kiminami, J. Magn.Mag. Mat., 256 (2003) 174.
[9] Prasad, S., and N. S. Gajbhiye, J. Alloy. Comp., 265 (1998) 27.
[10] Verma, A., T. C. Goel, R. G. Mendiratta, P. Kishan. J. Magn.Mat., 192 (1999) 271.
[11] Narayan A, R. K. Singh, M. Roy, B. Pandey, V. Kumar, H. C. Verma, Patna Univ. Jour. 31 (2007) 11.
[12] Albuquerque, A. S., Jose, D. Ardisson, Waldemar, A.A. Maedo, J. Appl. Phys. 87 (2000) 4352.
[13] Smit, J. and H.P.J. Wijn, Ferrites, (1959) Philips Technical Library, U. K. Edition, London. 145.
[14] Verma, A., T. C. Goel, R. G. Mendiratta, P. Kishan., J. Magn. Mag.Mat. 208 (2000) 3119.
[15] Caizer, C. and M. Stefanescu, J. Phys. D: Appl. Phys, 35 (2002) 3035.
[16] Coey, J . M. D., Phys. Rev. Lett. 27 (1971) 1140.

Corresponding Author:
Email: rakeshpu@yahoo.co.in

Manthan, International Journal, Vol. 12, June, 2011, Pages 12-15
ISSN No. 0974-6331 www.bbmanthan.info

Thermodynamical Properties of Inhomogeneous Associating Fluids Using Density Functions

Pradeep Kumar Choudhary

Department of Physics, R. D. S. College, B. R. A. Bihar University
Muzaffrapur 842002, Bihar, India

Abstract

An Analytical expression for molecular association on the phase coexistence properties of fluid with one or two direction attractive centre is discussed .The basic theory of Rosenfeld for the hard sphere is extended to inhomogeneous fluids on the basis of density function. The density functional approach in the grand canonical ensemble utilized to determine thermo dynamical properties of the inhomogeneous fluids. The theoretical prediction is in good quantitative agreement with the simulation result which is available

INTRODUCTION

The theoretical methods for predicting equilibrium properties of homogeneous non-polar fluids are now well documented; much less understood are the properties of confined associating fluids. The density functional theory is routinely used to investigate the properties of simple inhomogeneous system. For anisotropic association, molecular simulations are often computationally intensive and analytical theories give faithful representation of the local fluid structure[1]. The interplay between chemical association and in-homogeneity makes the phase behaviour of confined associating fluids interesting but difficult to predict.

For bulk associating fluids, Wertheim's thermodynamic perturbation theory provides a relative simple yet accurate description of thermodynamic properties

[6,8]. Most current applications of Wertheim's theory are limited to the first order perturbation that takes into account only the structure corresponding hard sphere reference system.

A quantity of central interest is the density functional theory has proven to be a theoretical approach in the study of inhomogeneous system [the] grand free energy Ω is written as a functional of the number density distribution $\rho(r)$.

2. BASIC THEORY

2 (a) Potential Model

We consider a binary mixture of neutral and associating hard spheres confined between two parallel hard walls. The pair-wise two body potential is given by

$$u(\mathbf{r}_{12},\omega_1\omega_2)= u_R((\mathbf{r}_{12}) + \sum_A \sum_B u(\mathbf{r}_{AB},\omega_1\omega_2), \qquad (1)$$

where $\mathbf{r}_{12}$ is the center to center distance between sphere 1 and 2, ω_1 and ω_2 represents the orientations of the two spheres, and the double sum applies over all associations sites. The reference potential u_R represents hard sphere repulsion is given by

$$u_R(r12)=\infty, \quad r_{12} < (\sigma_1 + \sigma_2) / 2 =0, \; r_{12} > (\sigma_1+ \sigma_2) / 2, \qquad (2)$$

where σ_1 is the hard sphere diameter for component i. The association potential u_{AB} represents the potential between a bonding site A on a spherical particle and a bonding site B from a different sphere with the condition when the attraction sites A and B on molecules 1, 2 prevents molecules 3 from coming close enough to form bond with either site A or B. The association potential is

$$u_{AB}(r_{12},\omega_1\omega_2) = -\varepsilon, \; r_{12} < r_c$$
$$= 0, \text{ otherwise} \qquad (3)$$

2 (b) Theory

Let us consider a model in which molecules are assumed to have one bonding site that allows for the formation of dimmers in the system, short ranged, highly anisotropic attractions are obvious choices as models for chemical bonding in the frame work of density functional theory (DFT). The grand free energy can be written as a function of μ_i.

$$\Omega(\rho_i(\mathbf{r})) = F(\rho_i(\mathbf{r})) + \sum_{i=1}^{3} \int d\mathbf{r}\rho_i(\mathbf{r})[\varphi_i(\mathbf{r}) - \mu_i] \qquad (4)$$

In an open system, the minimization of this grand potential at constant chemical potential μ_i, and absolute temperature T, determines the properties of the equilibrium states satisfies

Manthan, International Journal, Vol. 12, June, 2011, Pages 12-15
ISSN No. 0974-6331 www.bbmanthan.info

$$\partial\Omega/\partial\rho_i(r) = 0, \quad (5)$$

Hence Eqs.(4) leads to

$$\mu_i = [(\partial f_{hs}\rho_i(r))/(\partial\rho_i(r))] + [(\partial f_{bond}\rho_i(r))/(\partial\rho_i(r))] + \sum_{i=1}^{3}\int dr\,\rho_i(r)\varphi_{asso}(|r-r'|), \quad (6)$$

where $f_{hs}(\rho(r))$ denotes the local free energy density of a uniform hard-sphere density of a uniform hard-sphere fluid, $f_{bond}(\rho_i(r))$ corresponds to the local change in the free energy, $\varphi_{asso}(|r\text{-}r'|)$ is the attractive part of the isotropic association potential between particles and i=1,2,3. The Helmholtz free energy is expressed as contribution from an ideal gas terms and an excess term due to intermolecular interactions.

$$F(\rho(r)) = F_{id}\rho_i(r) + F_{ex}\rho_i(r). \quad (7)$$

The ideal gas contribution is given by the exact expression

$$F_{id}\,\rho_i(r) = kT\sum_{i=1}^{3}\int dr\rho_i(r)\{\ln(\rho_i(r)\lambda_i^3) - 1\}, \quad (8)$$

where $\lambda_i = (h/(2\pi\ mkT)^{1/2})$ represents the thermal wavelength. Here in a typical perturbation approach, the Helmholtz free energy for a system of inhomogeneous associating hard-sphere consists of hard sphere reference system and perturbation.

$$F_{ex}(\rho_i(r) = kT\int dr[\varphi_{hs}(\bar{\rho}_i(r) + \varphi_{asso}\{\rho_i(r)\}]. \quad (9)$$

Once we have an expression for the intrinsic Helmholtz free energy, solution to Eq.(5) gives the equilibrium density profiles and subsequently, thermodynamics properties. Equating the chemical potential of each component to that of the bulk fluid mixture of density (ρ_i^o) with which it is in equilibrium, the density distribution for the i^{th} component can be expressed as

$$\rho_i(\mathbf{r}) = \rho_i^0\exp[-\beta\varphi_i(\mathbf{r}) + c_i^{(1)}(\mathbf{r};[\{\rho_i(\mathbf{r}) - c_i^{\sim(1)}(\{\rho_i^0\})], \quad (10)$$

where $c_i^{(1)}(r;\{(\rho_i(r))\})$ is the one particle DCF of the i^{th} component, is defined as the functional derivative of the excess free energy functional $F_{ex.}$ i.e

$$c_i^{(1)}(r;\{(\rho_i(r))\}) = -\beta\,[\partial F_{ex}(\rho_i(\mathbf{r}))/(\partial\rho_i(\mathbf{r}))]. \quad (11)$$

The density Eq.(10) for the non-uniform fluid, on using the least particle method due to Percus, provides a route for the calculation of the RDF of the uniform fluid given by

$$g_{ij}(r) = \exp[-\beta u_{ij}(r) + c_i^{(1)}(r;[\{\rho_i^0 g_{ij}(r)\}]) - c_i^{\sim(1)}(\{\rho_i^0\})]. \quad (12)$$

Although Eqs.(10) and Eqs.(12) are formally exact for their practical implementation. The fundamental-measure theory of Resenfeld provides an expression for the excess intrinsic Helmholtz free energy density is represented as a function of weighted densities $\bar{\rho}_i(r)$

$$\bar{\rho}_i(r) = \sum_i\bar{\rho}_{\alpha,i}(r) = \sum_j\int \rho_j(r')\,\omega_{ij}(r - r')dr', \quad (13)$$

weights functions $\omega_{ij}(r)$, characterize the geometry of a spherical particle.

2 (c) Thermodynamic perturbation theory

Thermodynamic perturbation theory for mixture using the hard-core repulsive potential as the reference system and the second from perturbation as described in Eq.(9), therefore, the Helmholtz free energy density due to associations is given by

$$\varphi_{asso} = \sum_i M_{ij}\,\rho_j\,(\ln X_A - (X_B/2) + (1/2)), \quad (14)$$

where M_i is the number of association sites per molecule of species i, and X_A is the fraction of molecules of component i not bonded at site A. In Eq. (6.14) X_A is calculated from

$$X_A = 1/(1 + \sum_i\rho_j X_A\,\Delta_{ij}), \quad (15)$$

where

$$\Delta_{ij} = 4\pi\ g_{ij}^{hs}(\sigma_{ij}).\ f_{AB}.K_{AB}. \quad (16)$$

Here K_{AB} is a constant reflecting the volume available for bonding of the two sites on molecules 1 and 2, $f_{AB}=[\exp(\varepsilon/kT) - 1]$ represents the Mayer

function and g_{ij}^{hs} (σ_{ij}) is contact value of the hard-sphere pair correlation function for mixture.

$$g_{ij}^{hs}(\sigma_{ij}) = (1/(1-\xi_3) + (3\sigma_i\sigma_j/(\sigma_i+\sigma_j)\,\xi_2/(1-\xi_3)^2) + 2(\sigma_i\sigma_j/(\sigma_i+\sigma_j)^2\,\xi_2^2/(1-\xi_3)), \quad (17)$$

$$\xi_m = (\pi/6)\sum_{i=1}^{2}\rho_i\sigma_i^m), \quad (18)$$

where

$$m = 1,2,3 \text{ and } \sigma_{ij} = (\sigma_1+\sigma_2). \quad (19)$$

If i = j, for contact value of the pair distribution function of the hard core reference fluid is given by

$$g_{HS}(\sigma) = (1-\eta/2)/(1-\eta)^3. \quad (20)$$

Once we have an expression for the intrinsic Helmholtz free energy, minimization of the grand potential with respect to the density distributions Eq.(10) leads to the Euler Lagrange equation

$$\rho_i(r) = \Lambda_i^{-3}\exp[c_i^1[\mathbf{r},\rho_i(r)] + [\mu_i - \varphi_i(r)]/(kT)], \quad (21)$$

where $c_i^{(1)}[r;\rho_i(\mathbf{r})$ is the one particle direct correlation function, obtained from

$$c_i^{(1)}[\mathbf{r};\rho_i(\mathbf{r})] = -(1/kT)\{\partial F_{ex}(\rho_i(r))/\delta\rho_i(r)\}$$

$$= -\int dr' \sum_A \partial[(\varphi_{hs}+\varphi_{asso})/\partial\overline{\rho_i}(\mathbf{r})]\,\omega_{ij}.(r-r'). \quad (22)$$

At equilibrium, the chemical potentials of all species remain constant. When the confined fluid is in equilibrium with a bulk phase. The chemical potential can be calculated from

$$\mu_i = kT\ln(\rho_i + \Lambda_i^{-3}) + \mu_i^{ex,HS} + \mu_i^{ex,assoc.} \quad (23)$$

The first term of the Eq.(23) comes from the ideal gas, second term is the hard sphere and last term due to association chemical potential is calculated from Wertheim's thermodynamic perturbation theory. The bulk hard-sphere mixture characterized by the diameter ratio $\alpha = \sigma_1/\sigma_2$ with $\sigma_2 > \sigma_1$ the concentration $x = \rho_2^0/\rho_0$ with $\rho_0 = \rho_1^0 + \rho_2^0$ and the bulk packing fraction η is expressed as

$$\eta = \frac{\pi}{6}[\rho_1^0\sigma_1^3 + \rho_2^0\sigma_2^3]$$

$$= \frac{\pi}{6}[x + (1-x)\alpha^3]\rho_0\sigma_2^3. \quad (24)$$

The compressibility equation is given by

$$\beta P/\rho_0 = [(1+\xi_3+\xi_3^2)/(1-\xi_3)^3]$$

$$-3\eta_1 x(\frac{1}{\alpha}-1)^2[\{(1+\frac{1}{\alpha})+\sigma_2\xi_2\}/(1-\xi_3)^3], \quad (25)$$

where

$$\eta_1 = \frac{\pi}{6}\rho_1^0\sigma_1^3 = [(\pi/6)\{x+(1-x)\alpha^3)\}\rho_0\sigma_2^3]. \quad (26)$$

Since $\alpha = (\sigma_1/\sigma_2)$, and $\sigma_2 > \sigma_2$, therefore $\sigma < 1$. The value of

$$x = (\rho_2^0/\rho_0) \text{ and } \eta_1 = [(\pi/6)\rho_1^0\sigma_1^3], \quad (27)$$

RESULTS AND DISCUSSION :

In Fig.1.the calculated value of $\alpha(=\sigma_1/\sigma_2)$ plotted against $\Gamma\ (=\rho\sigma_2^3)$ at constant $\eta(=0.1)$ and $x(=\rho_2^0/\rho)$ at 0.1, 0.2, 0.3, 0.4, 0.5, and 0.6. The fig. shows the value of $x(=\rho_2^0/\rho)$ increases the corresponding value $\Gamma\ (=\rho\sigma_2^3)$ decreases and justify that the values approaches to where the ratio $x(=\rho_2^0/\rho)$ becomes 1.0.

In Fig.2 we have calculated the value of compressibility factor $\beta p/\rho_0$ with hard-sphere diameter ratio α=0.5 at constant mole fraction 0.25, 0.5, 0.75. The mole fraction ratio x increase the compressibility increases. The calculated results compared with available data of C. Barrio and J.R. Solana. The agreement is found good.

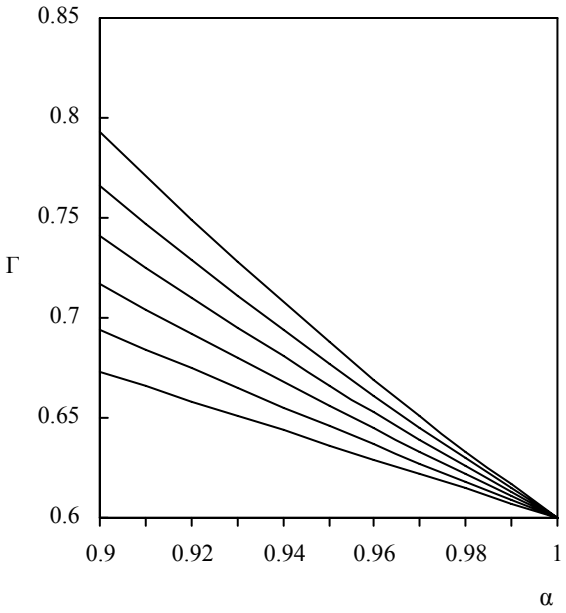

Fig.1 The value of Γ with respect to α at constant packing fraction and constant X

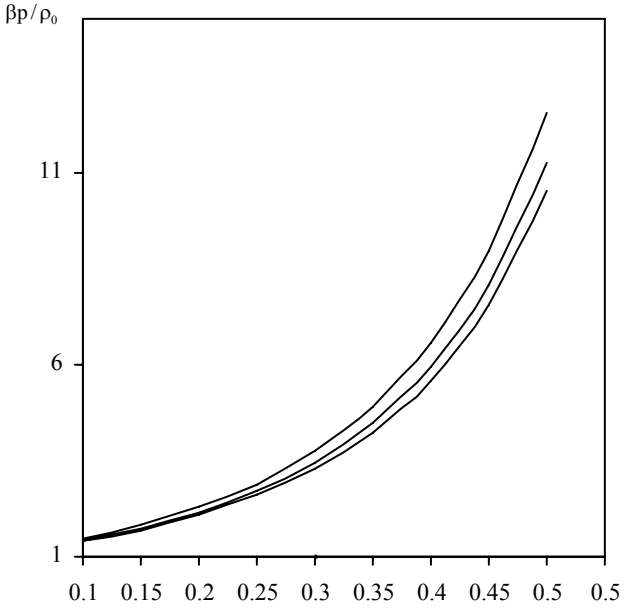

Fig.2 The compressibility factors for hard sphere mixture with diameter ratio constant value 0.5 with mole fraction 0.25, 0.5, 0.75.

References

[1] L.D Gelb,K E Gubbins, R Radhakrishnan and M Sliwinska Rep. Prog. Phys. **62** 1573 (1999).
[2] M S Wertheim J. Stat. Phys. **35** 19 (1984).
[3] M S Wertheim J. Stat. Phys. **42** 459 (1986).
[4] M S Wertheim J. Stat. Phys. **85** 2929 (1986).
[5] M S Wertheim J. Chem. Phys. **88** 1145 (1988).
[6] C J Seguno W.G Chapman and K P Shukla Mol. Phys. **90** 759 (1997)
[7] M F Holovko E Vakarin Mol. Phys. **85** 1057 (1995).
[8] G Jackson W G Chapman K E Gubbins J Chem. Phys. **65** 01 (1998).
[9] V Talanquer and D W Oxtoby J. Chem. Phys. **112** 851 (2000).
[10] Y Yang-Xin and W Jianzhong J Chem. Phys. **116** 7094(2002)

Correspondence Author:
Email: pkchoudhury1964@gmail.com

Manthan, International Journal, Vol. 12, June, 2011, Pages 16-19
ISSN No. 0974-6331 www.bbmanthan.info

Rejuvenating the Mathematical Morphology in Image Analysis

***Neha Gautam*[#], *Rahul Gaurav*[*]**

[#]*Department of Information Technology, Kuvempu University, India,*

[*]*Department of Electronics Engineering, Isik University, Turkey*

Abstract

Mathematical Morphology technique was first proposed in France in sixties for providing a very coherent theoretical framework for image processing and analysis.

This theory was receiving very little attention that time but nowadays, is becoming an object of research in many laboratories and international conferences. Recently, this tool has emerged as an important research topic as the image analysis field is expanding rapidly. Eventually, its impact has been evident by the specialist in the area of both spatial information theory and theories involved in digital image processing and analysis and others related to Mathematical Sciences as well.

The methodology used in this paper is likely to be useful for strategic analysis based on the mathematical theories of sets and topological notions, its principle lies in studying the morphological properties (shape, size, orientation etc.) of the objects through non-linear transformations associated with a reference object (the structuring element).

This paper presents a set theoretical approach and elucidates the basic concepts of the mathematical morphology in a rather general framework as the classical tool of analysis and segmentation of images. We will also identify some future research directions for mathematical morphology.

Mathematical Morphology: Image Analysis Perspective

This technique was initiated by G.Matheron and J.Serra for the quantitative analysis of spatial structures, at the Paris School of Mines.

If we break the term into two words then Mathematical does obviously refer to the mathematical part that is the use of set theory and morphology part refers to the study of shape. So in general we can say that Mathematical Morphology is a tool for extracting image components that are useful for representation and description. Its mathematical origins stem from set theory, topology, lattice algebra, random functions, stochastic geometry, etc. It helps us to perform automated measurements on image data. Thus, it involves set theoretic method of image analysis providing a quantitative description of geometric structures. It is most commonly applied to digital images, but it can also be employed on surface, surface meshes, graphs, solids and many other spatial structures. It characterizes various topological and geometric continuous-space concepts such as shape, size, convexity, connectivity and geodesic distance on continuous and discrete spaces. It is based on shapes in the images not the pixel intensities that are viewed as a general image-processing framework. Generally we use it before and after image segmentation (except the case of watershed segmentation). Two fundamental morphological operations – erosion (shrinking) and dilation (expansion) are based on Minkowski operations.

There are two different types of notations for these operations: Serra/Matheron notation and Haralick/Sternberg notation. In this paper, Haralick/Sternberg notation is used which is the more often used one in case of practical applications.

In this notation erosion is defined as follows (Eq. 1) (Serra, 1982):

$$X \ominus B = \bigcap_{y \in \hat{B}} X_y ,$$

and dilation as :

$$X \oplus B = \bigcup_{y \in B} X_y$$

Where, $X_y = \{x + y : x \in X\}$,

B and $B\hat{}$ are structuring elements and $\hat{B} = \{b : -b \in B\}$.

Manthan, International Journal, Vol. 12, June, 2011, Pages 16-19
ISSN No. 0974-6331 www.bbmanthan.info

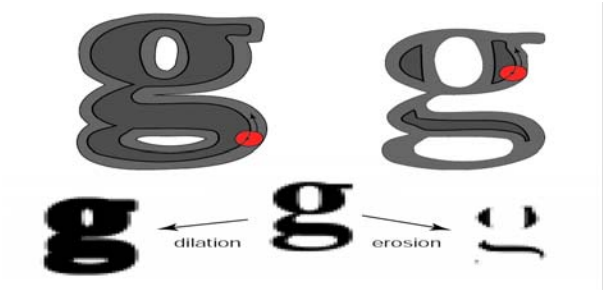

Fig 1 Dilation and erosion by a structuring element

There are two types of composites relations; one is called morphological opening and the other as morphological closing. The main aim of opening is to remove unnecessary structures in the image like noise. Binary opening removes the small regions that are smaller than the structuring element. It is defined as erosion followed by dilation and is given as an image F opened by a SE K:

$$O(F,K) = F \circ K = (F \$ K) \oplus K$$

Closing is used to merge or to fill the structure in an image. It is defined as dilation followed by erosion. It can fill the small holes that are smaller than the structuring element. Binary closing is an image F closed by a SE K is given as:

$$C(F,K) = F \bullet K = (F \oplus K) \$ K$$

Fig 2 Opening: remove capes, isthmus and islands smaller than the structuring element

Fig 3 Closing: fill gulfs, channels and lakes smaller than the structuring element

In the fig 1, it has been shown how morphological opening can remove a strip of land projecting into a body of water (capes), a relatively narrow strip of land (with water on both sides) connecting two larger land areas (isthmus) and island which are smaller than the structuring elements.
In the fig 2, filling of an arm of a sea or ocean partly enclosed by land (gulfs), channels and lakes small than the structuring elements has been explained.

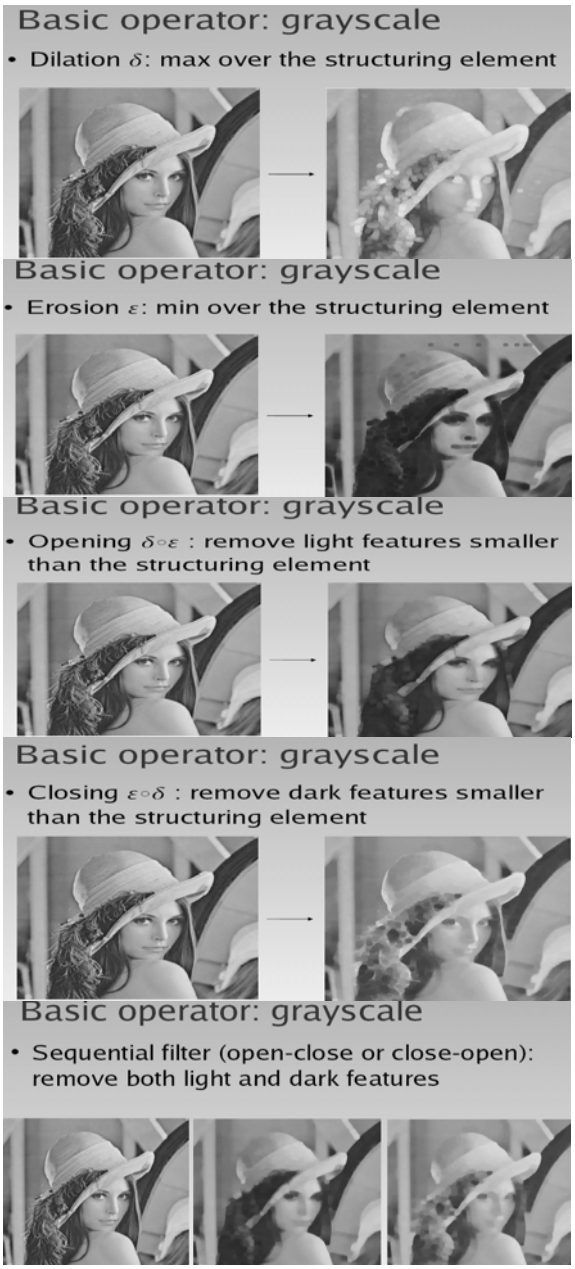

Fig 4 (a), (b), (c), (d) respectively

Future Work and Conclusion

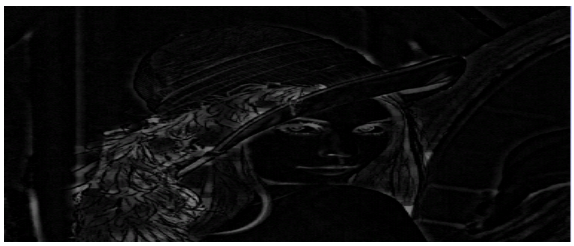

Fig 5: Black Top Hat: Closing (f) – f, "Extraction of Dark Features"

It is a powerful tool for solving various image related queries and also for such operations, which are difficult to be expressed, by other tools. MM helps us express such tougher operations in a rather easier way, such as the boundary extraction example. This approach is often used to post-process "threshold" images then performs some MM operations (like clean up noise, fill in holes) and as a result providing a nice segmented region.

The need for morphology has been evident in various fields of science and engineering as well which has been substantiated in recent years like the one in which it acts as one of the best methods to eliminate weak network lines so that there is an emergence of strongly connected sub-networks in such way that one can predict the behavior of the network. With the help of mathematical morphology, power network images are being decimated for analytical view. It gives a quick view of the strong sub-networks in the power system.

In the recent years, morphology has shown its need to the researchers in the realization of several topics like image enhancement, image segmentation, image restoration edge detection, texture analysis, feature generation, skeletonization, shape analysis, image compression, component analysis, curve filling, general thinning, feature detection and noise reduction.

It has shown directions to several researches and development works across the globe by providing an easier method in several image related applications. It helps in the teeth detection of a gear using subtraction and labeling, in getting the grid identification from Biochip by detecting the size of parts and analyzing its shape (pattern spectrum) using OTSU and entropy threshold. Another important application lies in the detection of runways in satellite airport imagery, which is a multi step algorithmic process that involves White Top-hat Transformation (segmentation tool that extracts respectively dark objects from the uneven background) of the source, image threshold and reconstruction of the detected long features to get the ultimate result. It's easy-to-use mathematical techniques have helped in the medical field too. In the detection of filarial worms, this tool has been proven to be the most efficient one. In such cases, Black Top-hat Transformation of source is firstly done [fig 5]. Hence the reconstruction after eliminating the short structures of the skeleton gives the final result.

In this paper, the applications and effectiveness of mathematical morphology was presented. The way, in which it is beneficial in dealing with many image-related problems, through various cited examples which were brought forth in a lucid manner. We saw the strength and versatility of this technique through the review of previous research works in this domain.

It has been rightly remarked by a famous researcher "though mathematical morphology is a powerful tool for many image analysis, it is not that famous because it is not useful or it is not used so it is not famous, may be because it involves too many mathematical theory!" but we saw the aspect in which it can be dealt with several image queries.

Hence, we conclude on this note of discussion that in spite of not gaining ample recognition, Mathematical Science, Geographic Information Sciences and image Science evidenced the efficiency of morphology and the time has come to prove its enduringness to the critics.

The crux of the matter is that we can await some more precise results in the world of images in the near future where the differences between the morphological and non-morphological operations will be well known to us

Acknowledgement

The authors would like to pay their gratitude to Mr Bibhuti Bikramaditya for his commendable support and valuable suggestions during the preparation of this paper.

References

1. Rahul Gaurav, "A Mathematical Morphological Perspective in the world of Images", *Seminar on Spatial Information Retrieval, Analysis, Reasoning and Modelling 18th-20 th March 2009. ISI-DRTC, Bangalore, India*
2. Hugues Talbot, "Image Analysis and Processing Mathematical Morphology" ESIEE – ECP 2006
3. Wyne Hsu, Mong Li Lee, Ji Zhang, **"**Image Mining: Trends and Developments", Journal of Intelligent Information Systems Volume 19, Issue 1 (July 2002).
4. William Green, "Edge Detection Tutorial." Internet:http://www.pages.drexel.edu/~weg22/edge. html, 2002. 3. M. Kowalczyk , P. Koza, P. Kupidura , J. Marciniak, "APPLICATION OF MATHEMATICAL MORPHOLOGY OPERATIONS FOR SIMPLIFICATION AND IMPROVEMENT OF CORRELATION OF IMAGES IN CLOSE-RANGE PHOTOGRAMMETRY", The International Archives of the Photogrammetry, Remote Sensing and Spatial Information Sciences. Vol. XXXVII. Part B5. Beijing 2008
5. Adrien Bousseau, "Mathematical Morphology a non exhaustive overview", pages 2-14.
6. Radhakrishnan, B. D. S.Sagar, and B. Venkatesh," Morphological Image Analysis of Transmission

Systems"IEEE TRANSACTIONS ON POWER DELIVERY, VOL. 20, NO. 1, JANUARY 2005.
7. Pierre Soille, Morphological Image Analysis. Springer-Verlag, 2003.
8. Rafael C. Gonzalez, Richard E Woods. Digital Image Processing. Prentice Hall, second edition, 2002.
9. Milan Sonka et. al. Image Processing, Analysis and Machine Vision. PWS Publishing, second edition, 1999.
10. Edge Detection using mathematical morphology, Neil Scott, RESEARCH CENTRE FOR INTEGRATED MICROSYSTEMS-UNIVERSITY OF WINDSOR, June 15th, 2007.
11. LIXU GU, SEMINAR SERIES ON ADVANCED MEDICAL IMAGE PROCESSING, LIXU GU, Robarts Research Institute London, Ontario, Canada, September 13, 2002
12. L. Najman, Using Mathematical Morphology for Document Skew Estimation, Laboratoire A2SI, Groupe ESIEE Cit´e Descartes, BP99.
13. Michael F. Goodchild, University of California, Santa Barbara, GEOGRAPHICAL INFORMATION SCIENCE FIFTEEN YEARS LATER, pages 2-4
14. Center of Mathematical Morphology (http://cmm.ensmp.fr/index_eng.html) at Ecole des Mines de Paris.
15. Morphology Digest (http://www.cwi.nl/projects/morphology) edited by Henk Heijmans, Centre for Mathematics and Computer Science, Amsterdam, The Netherlands
16. "Image analysis and mathematical morphology" by J. Serra (call# TA1632.S47 v.2 1988)
17. Ole Christian Eidheim," Introduction to Mathematical Morphology", Department of Computer and Information Science, NTNU
18. Shivprakash Iyer, Sunil K. Sinha J., 2005. Automated condition assessment of buried sewer pipes based on digital imaging techniques. Indian Institute of Science, Sep.–Oct., 85, 235–252

Corresponding Author:
Email: #neha.niitp@gmail.com
*rahulgaurav.kist@yahoo.com

Manthan, International Journal, Vol. 12, June, 2011, Pages 20-24
ISSN No. 0974-6331 www.bbmanthan.info

Identification Card Using RFID And Biometric Recognition

Bárbara Emma Sánchez-Rinza, Otto Hernández -González, Alonso Corona-Chávez**

*Benemérita Universidad Autónoma de Puebla, **Instituto Nacional de Astrofísica y Electrónica*
14 sur y avenida san Claudio Puebla, Pue. México

Abstract

In this work we show a system capable of identifying people from the fingerprint image, using an 8K RFID card that works wirelessly. The fingerprint images are processed through a series of techniques that improve their quality. From this template it is possible to verify the identity of the user with a95% accuracy.

I. INTRODUCTION

WITH the advance of technology, each day more and more tasks are performed in an automated fashion. Within the broad range of possibilities offered by technological development and innovation, we have observed that people authentication systems are becoming an emerging area, and consequently, biometrics is positioned as the focus of these systems. Biometrics refers to the use of distinctive anatomical traits (in this case fingerprints), called biometric identifiers, that can automatically recognize individuals. Biometrics is becoming an essential component of effective solutions for identification, because biometric identifiers can not be shared or lost, in addition to inherently represent the identity of the body of the individual. The recognition of a person's body is a very powerful identity management with enormous potential.

II.-FINGERPRINT

Fingerprints are fully formed around the seven months of fetal development and configuration of the edges of the fingers does not change during the life of the individual except due to some accidents such as scrapes or cuts. Moreover, they have the quality to be relatively stable over time. Therefore, the probability of finding two similar fingerprints is 1.9x10-15.
Today fingerprints represent one of the most mature biometric technologies. A fingerprint is the representation of the surface morphology of the epidermis of a finger. It has a set of parallel lines (ridges) which are formed before birth and remain without the time to generate some kind of change or modification [1] .

In this paper we use the Galton method for checking the local characteristics as it is one of the methods in which more work has been done and several algorithms exist with relatively low computational complexity.
The method of local characteristics is based on comparison of minutiae. Minutiae or Galton's characteristics (see Figure 1) are local discontinuities in the fingerprint pattern corresponding to the lines of the fingerprint. There are different types of minutiae, but the two most important are the bifurcations and terminations, as other types of minutiae are formed with a combination of both. For this reason, the feature extraction stage detects two types of minutiae [2].

Fig.1. Types of minutiae in a fingerprint.

To conclude whether two fingerprints match or not, the same person performs a procedure that begins with the classification of the fingerprint and matches the minutiae of both tracks.

III. BASE OF THE ACQUISITION

For an efficient biometric system, the indicators or personal traits under study must meet the following qualifications:

Permanence: the characteristic should not change with time, or do so very slowly.
Uniqueness: the existence of two people with identical property should have a very small probability. Universality means any person should have that feature.
Quantification: the property can be measured quantitatively [3].
The work was carried out following the steps shown in the diagram in Figure 2, which is explained below:

1.-Acquisition of the footprint that will be used to create the template which will be stored on the card.
2.-Image enhancement provide the benefit of having a better collection of minutiae.
3.-processing of images to extract some characteristic points, which represent the essential information of each track.
4.-Identification by comparing fingerprint minutiae stored in the card.

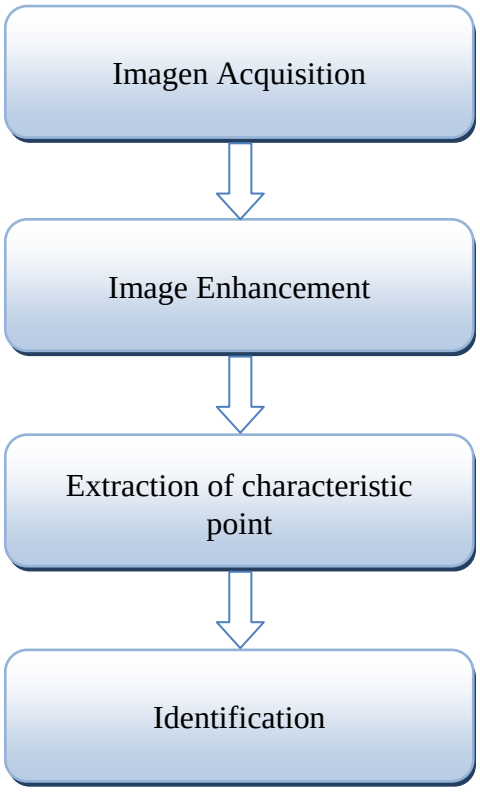

Fig. 2. Diagram of the steps that the system

IV ACQUISITION OF IMAGES

To get the image of the acquired fingerprint the "U.are.U4500 Person model" digital reader is used with the following characteristics (see Figure 3).
• Blue LED.
• Works well with dry or wet fingerprints.
• Compatible with Windows ® Vista, XP Professional, Windows Server 2000 and 2000, 2003, 2008.
• Pixel resolution: 512 dpi (on the scan area).
• capture area: 14.6 mm (width in the center) 18.1 mm (length).
• 8-bit grayscale (256 levels of gray).
• Reader size (approximate): 65 mm x 36 mm x 15.56 mm.
• Compatible with USB 1.0, 1.1 and 2.0 (High speed).

It was decided to use this model because of the quality of reading and friendly handling.

Fig. 3. Reader Digital Persona fingerprint mark.

Figure 4 shows tests performed with the reader to obtain fingerprints.

Fig. 4. Fingerprints acquired.

V IMAGE PROCESSING

The main objective of digital image processing is to extract a vector of characteristics that identify the individual. As mentioned above the method used for the comparison of fingerprints is with local characteristics [4]. Obtaining minutiae has been performed in 4 steps, as shown in Figure 5.

Manthan, International Journal, Vol. 12, June, 2011, Pages 20-24
ISSN No. 0974-6331 www.bbmanthan.info

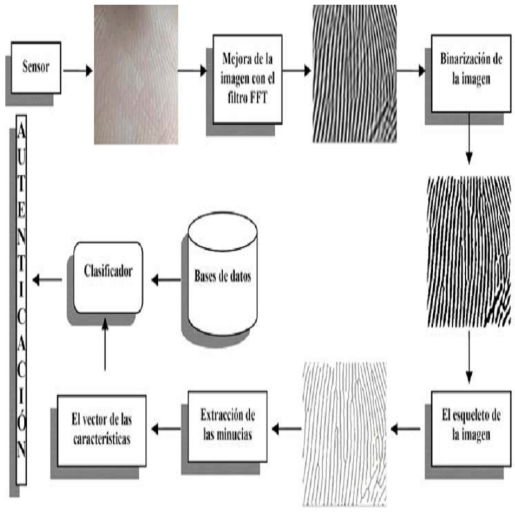

Fig. 5. Steps of the algorithm to acquire the feature vector.

The feature vector was obtained from the fingerprint image that was taken with digital fingerprint reader. These images have been digitally processed to enhance the minutiae. These lines form the descriptor of the fingerprint. A classifier based on a threshold and the Pearson correlation coefficient verifies whether a new mark belongs to the claimed identity. The results show a 95% confidence for a 50 people sample.

Defining information for the system. The first to be defined before the program was started, was the way in which data would be stored inside the card. It was decided that XML should be utilized because it allows that information to be stored and transferred from card system in a structured manner.

The way in which information is structured is shown in Figure 6.

```
<?xml version="1.0" encoding="utf-8" ?>
<Persona>
  <Nombre>OTTO HERNANDEZ GONZALEZ</Nombre>
  <CURP>HEGO830511HPLRNT04</CURP>
  <IFE>2001092134241</IFE>
  <ServicioMedico>SEGURO SOCIAL</ServicioMedico>
  <NoServicioMedico>001</NoServicioMedico>
  <Licencia>99999999999999</Licencia>
  <CartillaMilitar>123456789</CartillaMilitar>
  <Cedula>6242060</Cedula>
  <Informacion>NO ES ALERGICO A NINGUN MEDICAMENTO</Informacion>
  <Imagen>Foto.jpg</Imagen>
</Persona>
```

Fig. 6. XML File Structure.

Then, after having studied the concepts and algorithms behind fingerprints. the system programming is performed.

VI PROGRAMMING

For the realization of the system programming, C # language is employed because it facilitates interaction with the digital fingerprint reader and RFID card reader [5,6].

The first thing that works is the creation of the XML file, containing data information identifying the person. Figure 7 indicates the window where that s fingerprint images are captured. Due to the nature of the employed algorithms it is necessary to obtain four samples of the same footprint with the aim of obtaining better feature extraction footprint. Moreover, a photo and details of the person to be identified are added.

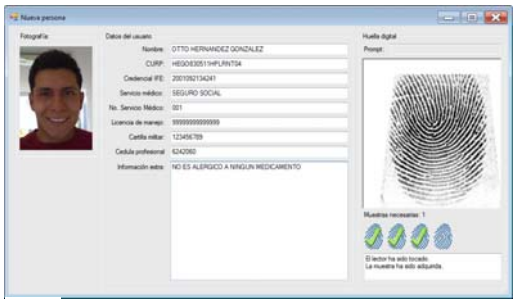

Fig.7. People capture window

The feature vector is stored in a file which is stored within the RFID card, which has a capacity of 8K and whose characteristics are:

•Mifare Model
• Frequency 13.56MHz
• Protocol ISO14443A
• 8192 Byte Size
• PVC Material

• Temperature -20 ℃ - +50 ℃

• Dimension 54 × 85.6 × 0.86 (mm)

To store information on it so it is necessary to take into account the size of the information is stored. Having the vector of features, validation is performed for people with their fingerprints, the first thing you need is to load the fingerprint template, the system returns a feature vector and compares it with the stored information for validation. Figures 8 and 9 show a positive and a negative validation.

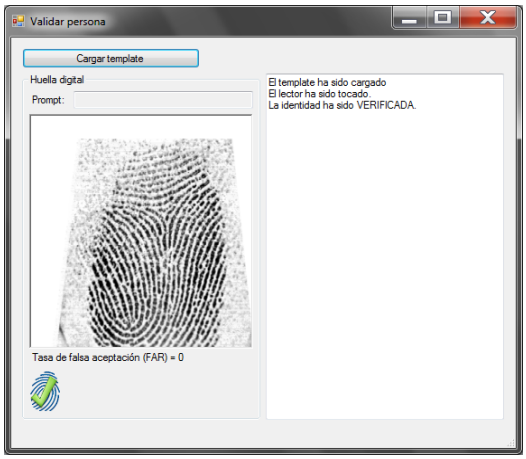

Fig. 8. Validation window with the person people validated.

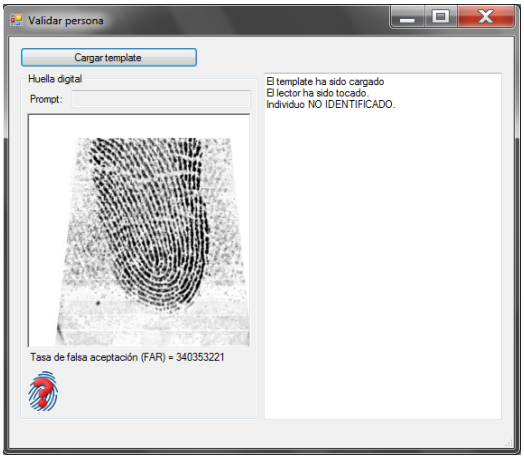

Fig. 9. People confirmation window with the person not validated.

Once the fingerprint validation is completed,m the RFID card is tested. The employed RFID system is as follows (see Figure 10):

• Model SL500
• Frequency 13.56MHz
• Protocol ISO14443A, ISO14443B, ISO15693
• USB Interface

• Temperature -20 ℃ - +50 ℃

• Dimension 110 × 80 × 26 mm
• Weight 100 g
• Windows System 98 \ 2000 \ XP \ NT \ ME \ Vista
• Maximum Range 5cm.

Fig. 10: RFID Card Reader.

As with the reading of the fingerprints it was decided to use programming language C # [7].

The following window has been created where the following operations are performed (see Figure 11):
• Connect the card reader
• Get the serial number on the card
• Read the information stored
• Write the information inside the card.

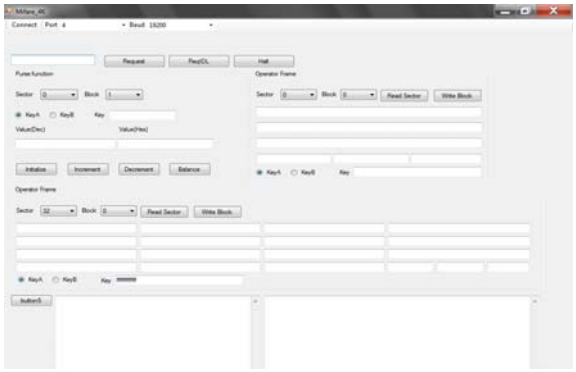

Fig. 11. Window for testing the RFID card

VIII CONCLUSIONS

In this work we have developed a system capable of identifying people from the fingerprint image, using an 8K RFID card that works wirelessly. The fingerprint images are processed through a series of techniques that improve their quality. From this template it is possible, with a classifier based on similarities to verify the identity of the user with a 95% accuracy. The future work is to encrypt the information of the person to protect sensitive data.

REFERENCES

[1] Davide Maltoni, Dario Maio, Anil K. Jain, Salil Prabhakar, "*Handbook of Fingerprint Recognition*", Springer, Año 2009
[2] Peter Komarinski, "*Automated Fingerprint Identificacion*", Elsevier, Año 2005
[3] Fabio Román Arbelo, Carlos Manuel Travieso González, Jesús Bernardino Alonso Hernández, "*Autenticación De Personas A Partir De La Biometría De La Región Dígito Palmar*", Vector plus: miscelánea científico – cultural, Fundación Universitaria de Las Palmas, Nº. 27, 2006, pags. 27-34
[4] Marius Tico, Pauli Kuosmanen, "*An Algorithm for Fingerprint Image Postprocessing*", Signals, Systems

and Computers, 2000, vol.2, Año 2000, pags. 1735 - 1739

[5] Klaus Finkenzeller, "*RFID Handbook: Fundamentals and Applications in Contactless Smart Cards and Identification*", Ed. John Wiley & Sons, Año 2003.

[6] Syed Ahson, Mohammad Ilyas, "*RFID Handbook: Applications, Technology, Security, and Privacy*", Ed. CRC Press, London New York, Año 2008, Páginas 13-15.

1. [7] Bill Glover and Himanshu Bhatt, "*RFID Essentials*", Ed. O'Reilly, Año 2006, 1-19.

Corresponding Author:
Email: brinza@cs.buap.mx

Manthan, International Journal, Vol. 12, June, 2011, Pages 25-28
ISSN No. 0974-6331 www.bbmanthan.info

High Efficient Solar Energy Harvesting System for Bihar Green Energy Initiative

Ranjan K. Behera

Department of Electrical Engineering
Indian Institute of Technology, Patna, Bihar, India

Abstract

As the cost of conventional energy sources continues to increase, alternative energy sources continue to gain in popularity beyond expectation and in this way to reduce environmental pollution. Alternative energy sources, such as Photovoltaic (PV) and Fuel Cell (FC), application is increasing day by day to meet the increased electrical load demand. Particularly, in stand-alone power supply system, powering the electrical load requirement and powering more number of electrical grids is one of the up-coming fields. In India especially in Bihar and Orissa, most of the rural areas are disconnected from the main power grid. Mostly it is in an isolated network, where electrical connection is impossible. To meet this power requirement in rural areas, the stand-alone PV system is the best choice. Although PV energy has received considerable attention over the last few decades, due to high installation cost and the low conversion efficiency of PV modules are the major obstacles to using this PV energy source on a large scale. Therefore, several studies are being developed in order to minimize these drawbacks of the existing system. In order to extract the maximum power of the PV array, the classical implementation of the maximum power point tracking (MPPT) in stand-alone systems is generally accomplished by the series connection of a dc–dc converter between the PV array and the load, the energy storage element or with a grid-tie inverter connected to grid. Considering that in the series connection, the dc–dc converter always processes all power generated, the total efficiency of the PV system greatly depends on the efficiency of this series dc–dc converter and grid-tie inverter. In order to improvement the system efficiency and reliability it is necessary to address suitable fault tolerant power electronics converters system for rural electrification. The power electronics converter topology should posses the ability of smart and intelligent load management and can be used for both isolated loads or grid connected system.

Introduction

With the ever-increasing demand for “green” energy, solar power has drawn a lot of attention by its rapid growth in recent years. It has been reported that worldwide solar system demand is predicted to continue to grow more than 30% annually for the next three years for the following reasons: excess manufacturing capacity has helped push down average photovoltaic (PV) system prices by more than 25%; the ongoing reduction of PV system installation cost; and the positive incentive movement in multiple regions [1].

Most of the isolated lands in India are situated on the hilly area where it is very difficult to install transmission line to those places due to high price and appreciable line loss. It is preferred to install a solar power generator at the consumers end or top of the hill. In these hilly areas there is plenty of sun shine. In fact, among solar generation system, those based on PV is one of the favorable and reliable method of the power generation for small size power module [2].

Due to rapid growth in semiconductor and power electronics technology, photovoltaic (PV) energy is of increasing interest in electrical power applications. The conventional two-stage PV energy conversion system includes a dc/dc converter and a dc/ac inverter that are connected between a PV array and an electrical power system [3]–[4]. The dc/dc converter is used to track the maximum power point of the PV array according to various maximum power-point tracking (MPPT) methods [5]–[7]. The dc/ac inverter is used to produce an output current in phase with the utility voltage and to obtain a unity power factor. However, the cost and efficiency of the two-stage PV energy conversion system are compromised because of the large number of individual devices, i.e., the dc/dc converter, batteries and dc/ac inverter. Hence, a single-stage PV energy conversion system is proposed for rural electricity applications, resulting in smaller physical volume, lower weight, lower cost, and higher efficiency [8], [9].

This paper aims to give an overview on grid connected PV inverters topology for rural electrification and to outline future trends in this rapidly developing technology. The paper is organized as follows. Section II describes solar power converter topology designs and discusses safety aspects concerning transformer less topologies. Section III outlines new developments including new system designs concept and discusses new transformer less

Manthan, International Journal, Vol. 12, June, 2011, Pages 25-28
ISSN No. 0974-6331 www.bbmanthan.info

topologies. Section IV summarizes the main findings and developments.

Solar Power Converter Topology

Power electronics design plays a key role in the performance of a solar power system, as design engineers first look at maximum conversion. Since PV modules have very low conversion efficiency from solar to electrical energy (in the range of 20 percent), the efficiency of a power inverter is meaningful to minimize solar module area and volume of the entire system. Additionally, power loss of devices generates heat on silicon dies that causes temperature rise and must be effectively dissipated. These losses lead to a thermal stress. Hence, a high reliable design of power electronics converter with heat sink is necessary. Minimum power loss not only saves energy, but also enhances system reliability, making the system more compact and less costly.

To convert the fluctuating direct current (DC) output voltage from solar modules into a well-regulated sinusoidal alternating current (AC) voltage, the architecture of a typical solar power conversion system is either two-stage or single-stage, with or without, DC/DC converter as shown in Figure-1 (a) and (b).

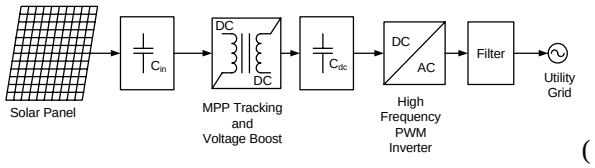

a)

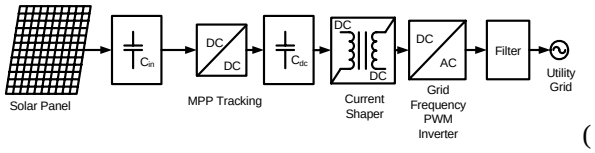

b)

Fig. 1(a-b): Grid connected classical solar power conversion system.

The existence of a DC/DC stage can maintain the input voltage of inverter at a constant and controlled level, and decouple the control of voltage and power flow. However, an extra conversion stage can have a negative effect on system efficiency. Because of this, more solar inverter manufacturers are evaluating and adopting single stage architecture, even when the inverter control is more complicated and voltage rating of power devices can increase. Among the recently introduced inverter topologies, two are considered to have the most potential for grid-tied centralized inverters in the future - HERIC (Sunways) and multilevel inverters. HERIC, shown in Figure 2, is structurally different than a conventional full-bridge inverter, incorporating an extra switch and diode pairs at the output. With these added devices and appropriate control, HERIC inverters are capable of boosting the system efficiency by effectively handling the reactive power flow.

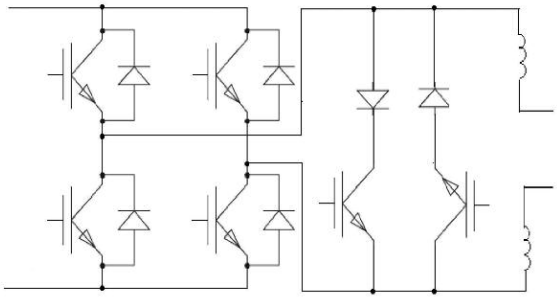

Fig. 2: HERIC inverter

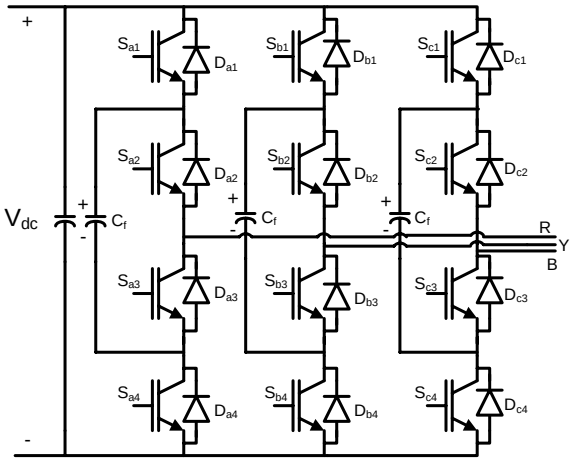

Fig.3: Three level neutral point clamped inverter.

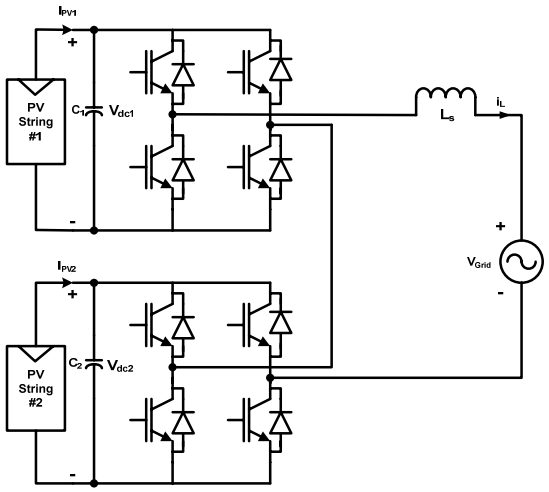

Manthan, International Journal, Vol. 12, June, 2011, Pages 25-28
ISSN No. 0974-6331 www.bbmanthan.info

Fig.4: Cascaded multilevel inverter.

Three level Neutral Point Clamped (NPC) and cascaded multilevel Inverter, shown in Figure 3 and Figure 4 is a specialized topology targeted at centralized solar power applications with higher voltages. Compared to its traditional counterpart, these inverters have only one half of voltage stress on each switch so that devices with much lower voltage can be used. This leads to higher efficiency and lower device costs. In addition, the electromagnetic interference (EMI) level and output filter size can be reduced, thus lowering the overall cost of the system.

Brief Description of the System

A simplified block diagram of the distributed power generating system for grid connected and isolated system by using a PV panel and a new storage device called energy capacitor system (ECaSS) is shown in Figure 5. The system is designed with an aim to meet a residential load of 1 kW peak, and the load pattern is assumed to have an average value of 530 W and a load form factor (LFF: the ratio of the total energy above the average power to the daily total energy) of 18% (as shown in Load-2 of Figure 8). Here, it is considered that the PV panel should be big enough to supply the peak power of the load. Its capacity is calculated using the following equation [10]:

$$E_{PV(min)} = P_{load} \times LFF \times 24 \quad (1)$$

where $E_{PV(min)}$: minimum daily output of PV panel (W·h);

P_{load} : average value of the load (W).

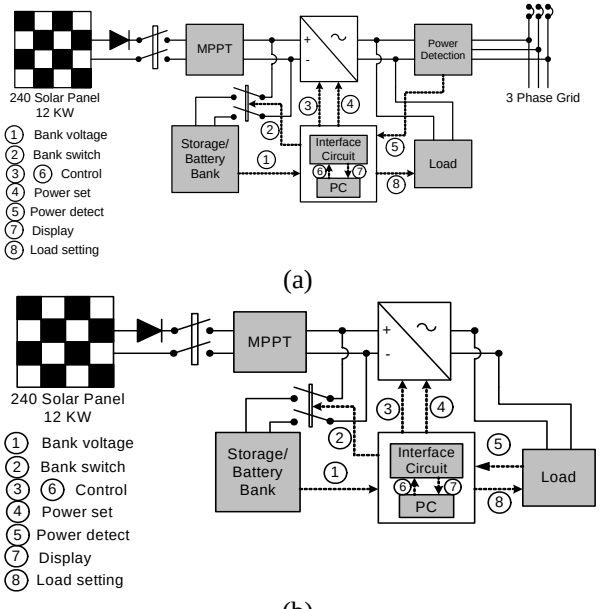

Fig. 5: Block diagram of the proposed rural electrification system. (a) Grid connected system (b) Isolated system

For the load mentioned earlier, (1) gives $E_{PV(min)}$ = 2.29 kW·h. As the load is ac, dividing this value by the efficiency of the inverter (=90%) we get, $E_{PV(min)}$ = 2.54 kW·h. To be on safer side, we have considered this value to be 3 kW·h. In Patna, Bihar, the minimum PV output is produced in the month of December. Using the estimation procedure discussed, it was found that a 1.2 kW panel could produce 3 kW·h/day in December. Hence, it is estimated that nine PV modules having a nominal V_{OC} of 24.0 V and I_{SC} of 7.69 A each. The modules can be connected in series that can produce a peak output of 1296 W at Maximum Power Point (MPP) (I_m = 7.2A, V_m = 180 V). Again, it is considered that the ECaSS should be big enough to supply the peak energy even during rainy days.

Estimation of PV Output Power

Once the insolation, incident on a PV panel, is known, its output power (PPV) can easily be estimated by the following equation:

$$P_{PV} = \mathcal{R} \text{ X } \cos\theta \times \eta_m \times A_p \times \eta_p \quad (2)$$

where $\mathcal{R}$ solar radiation (W/m2); θ angle of incidence calculated by considering $\beta = 45^\circ$

η_m efficiency of the MPPT = 96%;

A_p area of the PV panel = 8.505 m^2;

η_p efficiency of the PV panel = 11% (at 25◦C with a rate of change of −0.052%◦C).

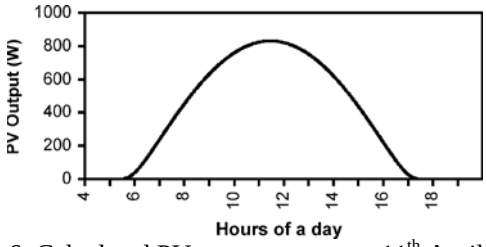

Fig. 6: Calculated PV output power on 11th April, 2010.

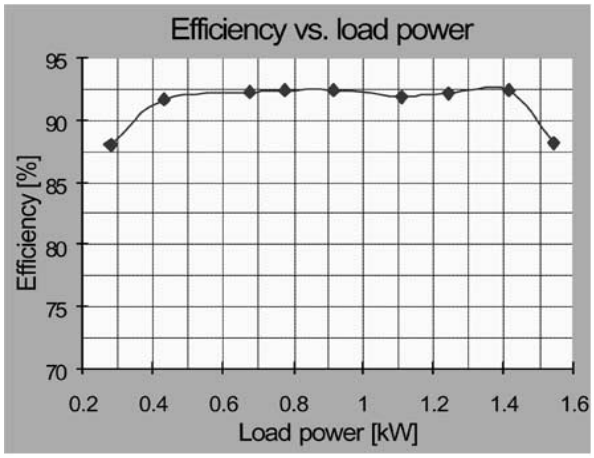

Fig. 7. Estimated efficiency versus load power

Considering the given values of the above parameters, the PV output on a typical sunny day has

been estimated and the actual output on the same day has been measured for comparison. The results are presented in Figure 6. Since, the value of η_p is calculated by considering the average temperature of the day, the estimated P_{PV} gives the temperature compensated value. The integrated energy of the estimated P_{PV} is 5.6 kW·h. Although the estimated PV output is smooth, the practically obtained one may have many fluctuations due to the tracking action of the MPPT. However, these fluctuations do not hamper the system operation. As the ECaSS can be charged and discharged quickly, it absorbs these variations and provides a steady output to the power conversion system (PCS). Estimated efficiency versus load power is given in Figure 7.

To study the performance of the system, three load profiles have been simulated. These are shown in Fig. 8. Among them, the first one is a typical commercial load, the second one is a typical residential load, and the third one is a hypothetical load pattern.

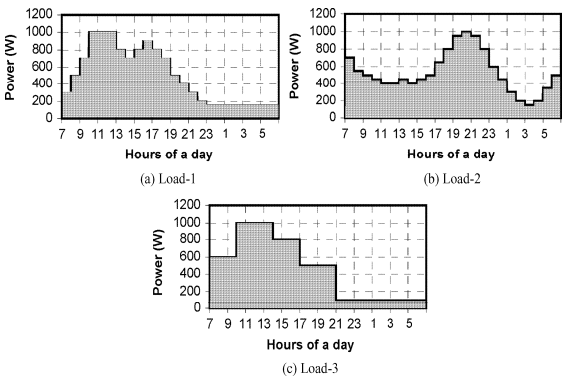

Fig. 8: Load profiles used for performance study.

Conclusion

The construction of a distributed power generating system of PV-ECaSS and its possible rural electricity generation have been presented in this paper. For its proper functioning, an estimation technique of the PV output power is also described. Using this estimated PV power the proposed system can work properly for Bihar green energy initiatives. The optimum power benefit and load-levelling facility can be achieved from the system with the help of the simulation program and the estimation of PV power. The obtained results prove the viability of the system. It is economically beneficial both in sunny days and cloudy days. In addition to the economical benefit, the system provides a good load-levelling feature. Moreover, the system has an excellent overall efficiency (92%) and is expected to be durable, as it is used the ECaSS that has longer lifetime than conventional batteries.

References

[1] C. Qian, “Solar Power Conversion – a System Solution to Alternative Energy Demand,” Application notes, Microsemi’s Power Products Group, Bend, USA, July 2010.

[2] B. K. Bose, P. M. Szczeny, and R. L. Steigerwald, “Microcomputer control of a residential photovoltaic power conditioning system,” *IEEE Trans. Ind. Applicat.*, vol. IA-21, pp. 1182–1191, Sept./Oct. 1985.

[3] S. J. Chiang, K. T. Chang, and C. Y. Yen, “Residential energy storage system,” *IEEE Trans. Ind. Electron.*, vol. 45, pp. 385–394, June 1998.

[4] H. Sugimoto and H. Dong, “A new scheme for maximum photovoltaic power tracking control,” in *Proc. IEEE PCC—Nagaoka’97*, 1997, pp. 691–696.

[5] J. H. R. Enslin, M. S.Wolf, D. B. Snyman, and W. Sweigers, “Integrated photovoltaic maximum power point tracking converter,” *IEEE Trans. Ind. Electron.*, vol. 44, pp. 769–773, Dec. 1997.

[6] C. Hua, J. Lin, and C. Shen, “Implementation of a DSP-controlled photovoltaic system with peak power tracking,” *IEEE Trans. Ind. Electron.*, vol. 45, pp. 99–107, Feb. 1998.

[7] K. H. Hussein, I. Muta, T. Hoshino, and M. Osakada, “Maximum photovoltaic power tracking: An algorithm for rapidly changing atmospheric conditions,” *Proc. IEE—Gen. Transmission Distrib.*, vol. 142, no. 1, pp. 59–64, Jan. 1995.

[8] A. Lohner, T. Meyer, and A. Nagel, “A new panel-integratable inverter concept for grid-connected photovoltaic systems,” in *Proc. IEEE Int. Symp. Industrial Electronics*, Jun. 1996, pp. 827–831.

[9] M. Meinhardt *et al.*, “Miniaturized low profile module integrated converter for photovoltaic applications with integrated magnetic components,” in *Proc. IEEE Applications Power Electron. Conf. Expo.*, Mar. 1999, pp. 305–311.

[10] R. Om, S. Yamashiro, R. K. Mazumder, K. Nakamura, K. Mitsui, M. Yamagishi, and M. Okamura, “Design and performance evaluation of grid connected PV-ECS system with load leveling function,” *IEEJ Trans. Power and Energy, Japan*, vol. 121-B, pp. 1112–1119, Sep. 2001.

Corresponding Author:
Phone No.: +91-612-2552050, 2277383 (Fax)
Email: rkb@iitp.ac.in

Manthan, *International Journal, Vol. 12, June, 2011, Pages 29-30*
ISSN No. 0974-6331 www.bbmanthan.info

Evolving Consciousness: from *Homo sapiens* to *Homo spiritualis*

Ranjeet Kumar

Central Drug Research Institute, Lucknow, India

The manifestation of that which exists but does not manifest is the progenitor of life. It's analogous to the seed which has potential of getting transformed in to a jungle. Transformation of the potential to kinetics is the key to origin and evolution. The whole purpose of life is precession as defined by Edward Hamming, it simply means that it's the effect of a body in motion on the other like throwing a stone generates ripples on the surface and perpendicular to it is the motion of the stone. Here the side effects at right angle to the motion matters and define the greatest philosophy behind a purposeful living. The true purpose of life is right angle to the goal we set. The goal of life is not the purpose as when you achieve the goal then you stop and there is no more precession. The central idea being that we should be in motion.

Initiating is important. The inherent mental inertia has been instrumental in limiting our capability to excel. There is always a fear factor at the back of consciousness that makes us uneasy in starting a new project. This is what mental programming all about. It's the nature and nurture factor that governs the ability to initiate and accept the consequences there after. A fast debugging of mental hard disk becomes inevitable. This world is truly for those who can quickly learn, unlearn and relearn under the dynamically changing environment. It's up on us to feed our grey matter with thoughts that are affirmative. Brain does not make any image of "no" what is needed is to come up with "yes" it's possible and I definitely can strive to achieve it. The script of success is written only when one knows the language of courage. As Paulo Coelho in his famous book says "When someone makes a decision, he is really diving into a strong current that will carry him to places he had never dreamed of when he first made the decision". So is what Swami Vivekananda has on this is "You fail only when you do not strive sufficiently to manifest infinite power". He strongly says that each soul is potentially divine and expressing this divinity in our thoughts and action is prime goal. The essence being that in the school called life you first take up the problem and later learn the lesson just opposite of what our conditioning and education has been.

The blueprint of perpetual happiness lies in the DNA of courage and the central dogma of life lies in the heart which drives you to an evolutionary roller coaster gradually transforming you from human doing to human being. Remember that the entire cosmos conspires when you inspired by naive thoughts desire to initiate. The essence being mind that is nothing but bundle of thoughts which keeps you in a state of confusion, and thoughts that can make difference get lost like needle in haystacks has to be brought to action. Become a strong magnet so that the needle does not get lost and prepare platform so that these small but important seeds with a potential to form jungles can be planted deep in to your consciousness that's what an idea can make tremendous difference all about. Let novel ideas perpetuate and does not let it die in gestation.

Mark Twain says "I have never let my schooling interfere with my education" this statement is quite pragmatic education to me is a lifelong exercise and sometime schooling create so much resistance in our thinking that we hesitate to initiate anything new. Deepak Chopra says that "every person is a god in embryo, its only desire is to be born" right indeed. What I want to convey in nutshell is that journey of thousand miles begin with a single step. So let every stone that comes your way become a milestone in your odyssey called life and not a tumbling hurdle.

What should have been a learning odyssey has become a painful pursuit for earning a living. Our education has ruined the capability of thinking innovatively and has definitely interfered with our learning process. Learning for the sake of knowledge that churns to what we called wisdom is no more happening. We have become so mechanized that the complexity of our mental faculty has left no room for creative thinking and enjoying the "being" part of our life. What I wish to propound is that in the struggle of existence "we are no more human being but human doing".

The faculty called mind is intricately complex and interesting entity. We can simply perceive mind as bundle of unorganized thoughts. What are these thoughts then, it's interesting that these are just like the trailing news that we always see on news channel most of which are breaking news and you know the element of truth is very little. "Breaking news" means that there is nothing positive or constructive, it's just there to break your calm conscious being. Most of your thoughts are programmed and there is no substance in

it. Being aware of the fact what can be done is to note those thoughts that are really worth pursuing this is analogous to finding needle in the hay sticks.

I don't know really whether I have made you comfortably miserable or miserably comfortable by putting my unorganized thoughts before you. But let me simplify the whole idea is to enjoy being what you are. I would like to give you a practical tip of becoming a banyan tree and not an ornamental bonsai. If you ask a seed about what's within it, the answer is nothing but remember this nothing is not the one we think it's a special nothing with an inherent potential of everything hidden in its core. So what if you plant the seed then a tree is born and that tree can breed numerous other trees and what would be the end result is a garden, a jungle. Likewise are our thoughts and what we need to do is to consciously plant these chosen thoughts in our subconscious mental field to prepare a customized tailor made garden of thoughts.

So let me share with you a technique called the pictographic technique that allows your desires to animate. It's a kalpvriksha its panacea for the holistic successful being. First think of something that you really want to achieve and seed this thought deep in to your subconscious being. After seeding the idea see the bigger picture, its meditation close your eyes and see the end result. Like if you seeded an idea of becoming a doctor, what you should see is that you are having a stethoscope with a batch on your chest that you are Dr. so and so. Seeing is important but imagine and dream take a bird's eye view attach intense emotion to the very thought, desire passionately and I bet if you go on doing this it will profoundly change your mental frame and you will automatically start attracting things that can make this happen Paulo Coelho the famous writer of Alchemist call it Natures Conspiracy but for me its map to your divine destiny. Now passionately desiring has to be converted in to your unflinching faith that yes if others can I can also and this is called transformation it's something sublime but will animate your faith in to action. Faith in action is important and it's driven by the fire within its similar to a small step in the right direction leading to a giant leap in your personal reality (personality). Suppose that you have always condemned rich friend of yours who owns a car and constantly pass negative comments. My only take home message is accept the things and stop kissing on negative note. Once you can accept the things in totality now let your faith work for you. The beauty of faith in action is it's scientific and it works the idea is whatever picture the brain see comes true. So let the brain be a nesting ground for noble ideas from nesting to testing from testing to investing from investing to creasting and crowning phase let your faith evolve step by step in the journey of wisdom.

Being is beautiful it's the canvas of God's masterpiece painting called life. Being let you get detached from the agony of the competitive living. Life has hidden musicality and there is every possibility that your being can let it surface on your personality. You get tuned to the vibes of almighty and the nectar flows. You become a dynamo of excellence driven by a purposeful living. I am concluding my write-up with the thoughts of Swami Vivekananda "Take up one idea. Make that one idea your life - think of it, dream of it, and live on that idea. Let the brain, muscles, nerves, every part of your body, be full of that idea, and just leave every other idea alone. This is the way to success that is way great spiritual giants are produced."

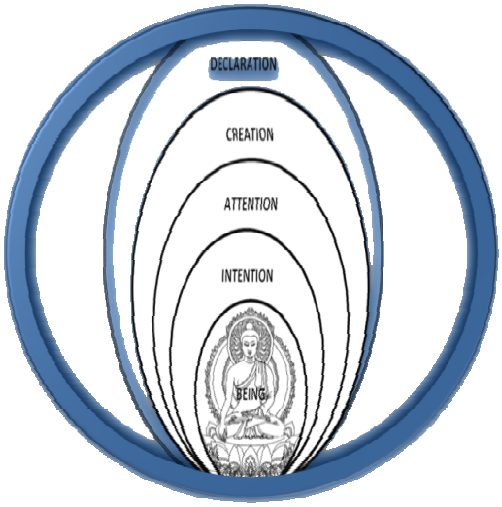

Conclusion

The ancient rule of Vedic connectivity is beautiful; it's a key to dynamic evolution of conscious positive being. It is manifestation of supreme energy and adding purpose to the divine existence of universal oneness.

Acknowledgement

The nature and nurture and all the saints and sages whom I have assimilated in my odyssey to truthful living.

Manthan, International Journal, Vol. 12, June, 2011, Pages 31-32
ISSN No. 0974-6331 www.bbmanthan.info

Plant Taxonomy in the Current Scenario of Molecular Biology and Bioinformatics

M. A. Ali

Department of Botany and Microbiology
College of Science, King Saud University, Riyadh, Saudi Arabia

Plant taxonomy is the science that finds, describes, classifies, identifies, and names the plants. Plant identification is the determination of the identity of an unknown plant by comparison with previously collected specimens or with the aid of books or identification manuals. The process of identification connects the specimen with a published name. Once a plant specimen has been identified, its name and properties are known. Plant classification is the placing of known plants into groups or categories to show some relationship. Plant systematics is involved with relationships between plants and their evolution, whereas plant taxonomy deals with the actual handling of plant specimens.

Modern biological classification has its root in the work of Carolus Linnaeus, who grouped species according to shared physical characteristics. These groupings since have been revised to improve consistency with the Darwinian principle of common descent. The traditional classification of plants into respective classes, orders, families, genera and species has been based on shared morphologic, cytologic, biochemical and ecologic traits. There are several approaches have been put forward time to time for classification of plants viz., form or habit of plant (Theophrastus, Caesalpino), artificial (Tournefort, Linnaeus), natural (Bauhin, Ray, de Jussieu, de Candolle, Bentham & Hooker) and phylogenetic (Engler & Prantl, Bessey, Hutchinson, Cronquist, Takhtajan, Thorne, Dahlgren, Angiosperm Phylogeny Group).

Since the 1960s a trend called cladistic taxonomy (or cladistics or cladism) has emerged, arranging taxa in an evolutionary tree. Molecular systematics or molecular phylogenetics which is an essentially cladistic approach and is the use of the structure of molecules to gain information on an organism's evolutionary relationships was pioneered by Charles G. Sibley (birds), Herbert C. Dessauer (herpetology), and Morris Goodman (primates), followed by Allan C. Wilson, Robert K. Selander and John C. Avise. Early attempts of molecular systematics were also termed as chemotaxonomy and made use of proteins, enzymes, carbohydrates and other molecules which were separated and characterized using techniques such as chromatography. Beginning in the early 1980s and continuing to the present, the use of DNA has represented the "cutting edge" (glamour area) within the entire field of plant systematics. Our understanding of the relationships among organisms at various levels in the tree of life has been advanced greatly in the last two decades with the aid of DNA molecular systematic techniques and phylogenetic theory. A diverse array of molecular techniques are available to the plant systematist for use in phylogentic inference, including restriction site analysis, comparative sequencing, analysis of DNA rearrangements (e.g. inversions), gene and intron loss, and various polymerase chain reaction (PCR) based techniques. These are generally considered superior for evolutionary studies since the actions of evolution are ultimately reflected in the genetic sequences. At present it is still a long and expensive process to sequence the entire DNA of an organism, and this has been done for only a few species. However, it is quite feasible to determine the sequence of a defined area of a particular chromosome. Closely related organisms generally have a high degree of agreement in the molecular structure of these substances, while the molecules of organisms distantly related usually show a pattern of dissimilarity. Molecular phylogeny uses such data to build a relationship tree that shows the probable evolution of various organisms. The most common approach is the comparison of sequences for genes using sequence alignment techniques to identify similarity.

Plant molecular systematics has relied primarily on the chloroplast genome. Nuclear ribosomal DNA is arranged in tandem repeats in one or a few chromosomal loci. Each repeat consists of a transcribed region that comprises an external transcribed spacer (ETS) followed by the 18S gene, an internal transcribed spacer (ITS-1), the 5.8S gene, a second internal transcribed spacer (ITS-2), and finally the 26S gene. Each such repeat is separated from the next repeat by an intergenic spacer (IGS). The nuclear genes that code for rRNA are repeated thousands of times within the typical plant genome. In fact they can comprise as much as 10% of the total plant DNA. The most remarkable feature of rDNA is the overall sequence homogeneity among members of the gene family in a given species. The process by which this pattern of intraspecific homogeneity and interspecific

heterogeneity is maintained has been called concerted evolution. It is widely accepted that in the process of concerted evolution a single mutation can be fixed in a relatively short time period due to unequal crossing over or gene conversion. These homogenization processes have been described as molecular drive. The coding regions show little sequence divergence among closely related species, whereas the spacer regions exhibit higher rates of variability. Therefore, nuclear ribosomal ITS sequence data have a great potential to resolve plant phylogenies at various intrafamiliar levels in angiosperms. Despite the large size of the nuclear genome, most attempts to infer phylogeny with nuclear gene sequences have involved the nuclear ribosomal DNA cistron (rDNA). The approximate lengths of the three coding regions are very similar throughout plants. The 18S gene equals 1,800 bp, the 26S gene equals 3,300 bp, the 5.8S gene equals 160 bp. In contrast, the length of the IGS varies considerably (from 1 to 8 kb). This variation in IGS length is the major contributors to the large range of variation in total length of the repeat unit in plants, ranging from approximately 8-15 kb. Variation in the length of the ITS-1 and ITS-2 regions is also noteworthy. The external transcribed spacer (ETS) region (especially the 3'end of the 5'-ETS adjacent to 18S) has sometimes been exploited in lower-level phylogenetic analyses. The nuclear genome of plants consists of certain DNA sequences that are present once per genome. These are referred to as single copy or unique sequence DNA. The lengths of single copy sequences in plant genomes usually vary from 200 to several thousand bp. Single or low-copy nuclear genes have also great potential to elucidate phylogenetic relationships of plants. The advantages of nuclear genes include the availability of many genes, their overall faster rate of evolution, and their biparental inheritance.

As gene sequencing becomes easier and cheaper, molecular systematics is being applied to more and more groups, and in some cases is leading to radical revisions of accepted taxonomies. The term bioinformatics is most commonly associated with the analysis of data generated by molecular biology. Genomics, the study of the nucleotide sequence of organismal genomes, and proteomics, the record of all proteins produced by a genome, are viewed as the frontiers of bioinformatics. The informatics challenge in these fields is turning the vast amounts of genomic and proteomic data into understandable and useful information. Development of phylogenetic theory and cladistic analysis of DNA sequences data has resulted into phylogenetic classification of the land plants. DNA barcoding -the use of short DNA sequences for biological identifications has gained worldwide attention in the scientific community which revolutionizes our knowledge of plant diversity and is on its way to being accepted as a global standard for the purpose of species identification.

India, with its wide range of physiographic and climatic conditions, has a rich varied flora, unparalleled in any other country in the world. The physiographic diversity of the country has produced all possible types and extremities of climatic conditions suitable for supporting wide varied types of ecosystems. It is estimated that about 45,000 species of plants which forms the conspicuous vegetal cover comprises about 6.8% of all known flowering plants of the world. With 2.46% of land area having 6.8% of flowering plants, India is recognized as one of the top 12 mega-biodiversity centers of the world. However, the Indian plant taxonomist is still cataloguing the life even in the era when Plant taxonomy is being practiced using tools and techniques of molecular biology and bioinformatics. The molecular systematic studies in India on Indian flora is in infancy due to lack of proper training of molecular biology and bioinformatics especially to taxonomist, thus a rich biodiversity of India has remained untouched from molecular systematic studies and in understanding the evolutionary relationship. There is thus an urgent need to review the status of taxonomic studies in India in context with latest development in the discipline. With the rich biological resources and many outstanding botanists who are familiar with the regional flora and interesting systematic questions, should initiate molecular systematic program to advance our understanding on the tree of life and to address new evolutionary questions.

Correspondence:
Phone: +966-4677561
Email: majmalali@rediffmail.com

Manthan, International Journal, Vol. 12, June, 2011, Pages 33-34
ISSN No. 0974-6331 www.bbmanthan.info

Resurgence of Infectious Diseases and Emergence of New Infections

Diwakar Tejaswi

Consultant Physician & Medical Director, International Health Organization & PAHAL
Exhibition Road, Patna-800001, Bihar, India

The environment influences our health in many ways - through exposures to physical, chemical and biological risk factors. Globally, nearly one quarter of all deaths and of the total disease burden can be attributed to the environment.

Over the last 30 years the reversal in the declining death rate due to infectious diseases has alarmed international health experts. Dramatic successes in eradicating small pox, controlling polio and tuberculosis, and eliminating vector-borne diseases such as yellow fever, dengue and malaria from many regions convinced most experts the era of infectious diseases would soon be over. Unfortunately this optimistic prognosis was premature as a number of diseases have dramatically reemerged. Tuberculosis (MDR and XDR TB), cholera, dengue, plague, and malaria have increased in incidence or geographic range, as have new drug-resistant strains of bacteria. In addition newly recognized diseases, such as AIDS or H1N1, have emerged.

The present global emergence of infectious diseases is clearly associated with the social and demographic changes of the past 50 years, particularly urbanization and globalization, with the attendant spread of pathogens (agents causing disease) via infected humans, hosts, vectors or commodities. The change in the environment caused by human activities is also apparent in the transformation of much of our landscape and conversion of regional systems once dominated by natural ecosystems. Factors include expansion into urban or peri-urban habitat, deforestation, and the spread of intensive farming. The environment's role in the emergence of diseases is apparent in the connections between the direct consequences of human changes to urban and rural landscapes and ecosystems, and the secondary effects on disease emergence factors. Developing irrigated agriculture, for example, can create breeding grounds for mosquitoes, a vector for malaria. Likewise the inadequate storm drainage and sewerage systems often associated with rapid urbanization not only increase the breeding habitat for disease vectors but facilitate the spread of waterborne pathogens causing cholera and leptospirosis.

Overwhelming evidence points to human demographic changes as the major direct and indirect factor contributing to the increase in infectious disease, with somewhat different dynamics and mechanisms at work in urban and rural environments. In the first case the increasing number of people crowded into dense settlements has dramatically increased opportunities for food, water, rodent and vector-borne pathogens to "colonise" and persist in human populations. Each pathogen has unique transmission and adaptive characteristics that determine a minimum population for survival (the threshold for measles is about 250,000 people). Whether the threshold is 100,000 or a million the number of large urban settlements and the average settlement size has been growing fast in recent decades. The number of cities of one million or larger was 76 in 1950, 522 in 1975, and 1122 in 2000, and is set to exceed 1600 by 2015. This 20-fold increase translates to a roughly similar increase in global infectious disease vulnerability due to this one factor alone.

This type of growth has indirect social and environmental consequences that contribute to multiplying the actual increase in population. Poverty, poor living conditions, including lack of sanitation and infrastructure for waste-water and solid waste management, increases opportunities for vector- borne diseases and others passing from animals to humans. The geographic spread and expansion into peri-urban areas of the mosquito *Aedes albopictus*, exquisitely adapted for breeding in discarded plastic containers and used automobile tires, is a good example of how a potential vector of viral diseases has taken advantage of environmental change. Lack of sanitation and waste water treatment, and industrial scale intensification of animal production systems the world over; contribute to exotic species, and the proliferation and spread of water and food-borne pathogens. Increasingly frequent outbreaks of infections are caused by these and other organisms, many of which may eat alongside or prey on wild mammals and birds as natural parasites. The contamination of surface waters and spread of pathogens is further promoted by the alteration of catchments and watersheds accompanying urbanization, and intensive farming around cities. Channeling streams, removing vegetation on the banks, and filling in wetland - all of which accompany unplanned urbanization - eliminate the natural retention and nutrient recycling systems, as well as

barriers to surface run-off contaminated with intestinal pathogens. Nutrient pollution leading to oxygen depletion in estuaries, lakes, streams and even stretches of ocean, such as the Gulf of Mexico, helps such pathogens survive too.

In rural areas population and consumption play a less direct role in contributing to disease emergence, particularly as rural emigration is fuelling the demographic explosion in cities. It is more that urban areas are driving a sustained increase in the timber trade, agriculture, stock raising and mining, resulting in turn in deforestation and changes in land use that are transforming rural landscapes and natural areas in ways that often facilitate the emergence of disease. Deforestation or even "patchy" reforestation leads to ecological changes such as increased edge habitat and local extinction of predators that favour some disease vectors and reservoir species. Encroachment of individuals and settlements on natural ecosystems brings humans into contact with known and novel pathogens. The spread and intensification of farming results in the development of irrigation systems, ideal breeding sites for mosquitoes and a habitat for opportunistic insects and rodents that may be vectors or reservoirs for disease. Dams provide a favorable habitat for other vectors.

Climate change represents a potential environmental factor affecting disease emergence

Shifts in the geographic ranges of hosts and vector, the effect of increasing temperature on reproductive, development and mortality rates on hosts, vectors, and pathogens, and the effects of increased climate variability on flooding and droughts all have the potential to affect disease incidence and emergence positively or negatively. At present there is insufficient evidence to indicate what the net effect will be once climate changes begin to have a major affect on ecosystems. However, a dominant theme emerging from research on the ecology of infectious disease is that accelerated and abrupt environmental change, whether natural or caused by humans, may provide conditions conducive to pathogen emergence: pathogen adaptation, host switching, and active or passive or dispersal.

The resurgence of infectious diseases worldwide reflects our quick-fix mentality, with poor development planning, a lack of political determination and institutional inertia. It is not the inevitable result of development, environmental change, or even incremental population growth. On the contrary much can be done to reverse the current trend. As well as rebuilding the public health infrastructure for infectious diseases, there is substantial evidence and a growing number of examples of how regional planning and development, including urbanization, agricultural expansion, and the management and conservation of forests and other ecosystems can minimize and even reduce outbreaks of infectious disease as well as environmental damage. Basically we need an integrated approach to pathogen control. This approach will involve meshing social and economic development programs, environmental and natural resource management, with intervention based on the reinvigorated field of disease ecology and methods involving community participation.

Correspondence:
Phone: 91-612-2206964, 91-9835078298(M)

Manthan, International Journal, Vol. 12, June, 2011, Pages 35-36
ISSN No. 0974-6331 www.bbmanthan.info

Water Scarcity Issues in Bihar, India

Ashok Kumar Ghosh

Department of Environment and Water Management, A.N. College, Patna, Bihar, India

Increasing global temperature has caused widespread glacier recessions in the new fold mountain belts of the Himalayas. Glacial recession has affected the flow of the Ganga river system, its impact being enhanced by human interventions. There are many adverse impact of the current climate change on the drainage pattern and river ecology of the Ganga system in Bihar (India). A rapid shift in the river meander occurred along Patna within a span of a few years. The reduced volumes of river water are leading to ecological disaster in Bihar in the form of truncated channel flows, and increasing sedimentation. This, along with pollution load, has aggravated aquatic life, as revealed in large-scale herniation in the zooplanktons. Also, abrupt drop in the river depth was indicative of local faults along the river bed, implying seismic impacts of ongoing changes in the river's regime. Our studies have concluded that climate change, apart from affecting life forms, was also altering the geomorphology of the Ganga Basin in the state of Bihar.[1]

The northern part of the state of Bihar, India, has innumerable south flowing streams that are subject to annual inundation. The river basins bear numerous water bodies and marshy lands. A systematic study of wetlands of north Bihar was undertaken by our research group for the period 1984 –2004 through remote sensing data. The observations are very interesting and alarming. Rapid changes in surface water regime have been detected. There is a contradictory trend in eastern and western parts of the study area, the former showing expansion of surface water and the latter revealing rapid shrinkage of the same.[2]

Testing of groundwater used for drinking for arsenic has been undertaken more widely by our research group in several districts of Bihar with the support of UNICEF. Available data for sixteen districts are collated which provides the most up-to-date picture of areas known to be affected by arsenic in groundwater in the Indian portion of the Ganges-Brahmaputra river basin. Bihar is one of the states where the ground water is heavily contaminated with arsenic. In Bihar, on the River Ganges upstream of West Bengal, 66,623 sources from 11 districts have been tested and water samples from 10.8% of sources were found to contain arsenic at concentrations greater than 50 μgL−1 and 28.9% at concentrations greater than 10 μgL−1.[3]

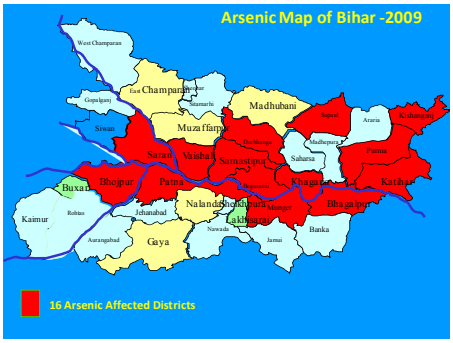

Fig. 1: Arsenic affected districts of Bihar

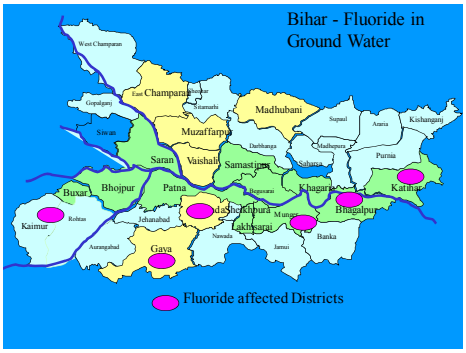

Fig. 2: Fluoride affected districts of Bihar

There is a proven correlation between high iron and high arsenic concentrations. In Bihar, majority of the arsenic hotspots found to be distributed in HCO_3 – dominated ground water facies. Contrary to our preliminary assessment that arsenic hotspots clustered along the banks of the master stream, Ganga, the interfluvial terrain and Himalayan foothills in north Bihar also tested positive for arsenic contaminated ground waters, the latest concentrations being detected in Darbahanga - Purnea Belt and the Kishanganj - Supaul Terai belts. Hence, arsenic contaminations occur continuously from the northern foothills to the south Ganga Plains, with the typical spatial variations in contamination levels within short distances. General arsenic concentrations also recorded to be decreasing with increasing depth, with the sole exception of western Bhojpur district where shallow

aquifers had less arsenic levels than the progressively deeper ones. Highest concentration of 1861 μgL−1 was recorded in this district, where out of 5420 hand pumps surveyed, 45% hand pumps had more than 10 μgL−1 arsenic. In Bhagalpur district 4516 hand pumps were surveyed, out of which 24.78 % had more than 10 μgL−1 arsenic. A large number of biological samples tested positive for arsenic toxicity. The study is still going on in several districts and the complete picture is yet to emerge in some areas. Deep groundwater in particular requires a comprehensive programme of supporting research to determine appropriate aquifers and ensure aquifers tapped remain safe from arsenic in the longer term. In this and other respects continued monitoring of groundwater quality in arsenic-affected areas is of the utmost priority.[4]

Fluoride contamination is another serious problem related to ground water of Bihar. Isolated pockets of intense fluoride contaminations have been found in the southern districts of Nawada [maximum 15.6 ppm], Gaya, Rohtas, and Munger and southern Bhagalpur district. Study of fluoride contaminations are in progress, the identified areas having aquifers at fluctuating levels and limited surface water resources in contrast to the northern water surplus districts. Villages with fluoride contaminations include Bhoopnagar and Masuribarof Amas Block, and, Bhaktauri, Kamalpur and Dhaneta of Bankebazar Block [Gaya District]; Rajauli, Kachariyadih and Muslim Tola [Nawada District].[5]

All the studies undertaken by our research group related to water quality and quantity indicate that the state of Bihar is going to face serious water scarcity in near future. Water crisis will become endemic in this water surplus state and urgent remedial measures are required to preserve and protect this precious water resource essential for our survival.

References

[1] Ghosh et al., (2007) Global Warming and changing land use patterns in Bihar Plains, India. In: Proceedings of Annual Conference of Royal Geographical Society, London.

[2] Ghosh et al., (2004) The Impact of Changing Surface Water Configuration on Land use of Bihar, India. In: Proceedings of ISCO 2004 Conference, Brisbane, Australia.

[3] Nickson et al., (2007). Current knowledge on the distribution of arsenic in groundwater in five states of India. Journal of Environmental Science and Health, 42: 1–12.

[4] Ghosh, A., N. Bose, A.G. Bhatt and R. Kumar (2010) New dimensions of groundwater arsenic Contamination in Mid-Ganga Plain, India. Arsenic in Geosphere and Human Dimensions-As 2010 CRC Press, UK.

[5] Ghosh, A., S.K. Singh and N. Bose (2009) Monitoring and Management of Arsenic and Fluoride Contamination in Ground Water of Bihar [India]. In: Bangladesh Chemical Congress, University of Dhaka, Bangladesh, pp15-16.